Available online at www.sciencedirect.com
SCIENCE DIRECT®
Coordination Chemistry Reviews 241 (2003) 273–294
COORDINATION CHEMISTRY REVIEWS
www.elsevier.com/locate/ccr

Annual survey of organometallic metal cluster chemistry for the year 2001

Michael G. Richmond *

Department of Chemistry, Center for Organometallic Research, University of North Texas, Denton, TX 76203, USA

Accepted 15 October 2002

Contents

Abstract . . . 273
1. Dissertations . . . 273
2. Homometallic clusters . . . 274
   2.1 Group 6 clusters . . . 274
   2.2 Group 7 clusters . . . 274
   2.3 Group 8 clusters . . . 275
   2.4 Group 9 clusters . . . 282
   2.5 Group 10 clusters . . . 283
   2.6 Group 11 clusters . . . 285
3. Heterometallic clusters . . . 285
   3.1 Trinuclear clusters . . . 285
   3.2 Tetranuclear clusters . . . 288
   3.3 Pentanuclear clusters . . . 289
   3.4 Hexanuclear clusters . . . 289
   3.5 Higher nuclearity clusters . . . 290
Appendix A . . . 291
References . . . 291

Abstract

The synthetic, mechanistic, and structural chemistry of organometallic metal cluster compounds is reviewed for the year 2001.

Keywords: Organometallic metal cluster compounds

1. Dissertations

The use of $Ru_3(CO)_{12}$ as a CVD precursor for the construction of bilayer and alloy films of Ru and Pt or Pd has been studied. Interlayer diffusion has been confirmed in the Ru | Pt and Ru | Pd bilayer films, with XRD data revealing the existence of a mixture of hexagonal ruthenium and cubic platinum/palladium phases in the films [1]. The mechanisms of electron transfer and hydrogen activation in a series of triruthenium clusters have been investigated. In the case of the cluster compound $H_2Ru_3(CO)_8[\mu\text{-}P(^tBu)_2]_2$, the kinetics and mechanism for reversible H_2 addition across one of the Ru–Ru bonds are described [2]. A study involving the reaction of rhenium carbido carbonyl clusters with electrophiles from the Group 12 metals has been published. The reaction of $[Re_7C(CO)_{21}]^{3-}$ with $Hg(NO_3)_2 \cdot 2H_2O$ affords the bridged dimercury(I) cluster $[\{Re_7C(CO)_{21}Hg\}_2]^{4-}$, whose X-ray structure confirms the presence of a $\mu_3,\mu_3\text{-}Hg_2^{2+}$ moiety. The details associated with the chemical oxidation of this cluster are presented and the resulting products are discussed. The reaction between $[Re_7C(CO)_{21}HgCl]^{2-}$ with L-cysteine yields $[Re_7C(CO)_{21}HgSCH_2CH(NH_3)(CO_2)]^{2-}$. This reaction is discussed relative to the use of this starting

* Tel.: +1-817-565-3548; fax: +1-940-565-4318
E-mail address: cobalt@unt.edu (M.G. Richmond).

0010-8545/02/$ - see front matter
PII: S0010-8545(02)00297-7

cluster as an electron dense, easily detectable label for sulfhydryl sites in proteins [3]. A dissertation dealing with the synthesis and characterization of high-nuclearity Group 10/11 heterometallic clusters has been published. Some of the clusters prepared and structurally characterized include $[Au_{16}Ni_{24}(CO)_{40}]^{4-}$, $[Au_{27}Ni_{40}(CO)_{56}]^{4-}$, and $[Au_6Ni_{30}(CO)_{42}]^{2-}$. The cyclic voltammetric behavior and spectroscopic data (NMR and EPR) of these clusters are presented and discussed relative to suitable bonding models. Also reported is the chemistry of the non-stoichiometric, trimetal clusters $[Au_6Pt_6(Pt_{6-x}Ni_x)Ni_{20}(CO)_{44}]^{6-}$ (where $x = 2.9–5.1$), which are isostructural with the known clusters $[Au_6Pd_6(Pd_{6-x}Ni_6)Ni_{20}(CO)_{44}]^{6-}$ (where $x = 2.1–5.5$) [4].

2. Homometallic clusters

2.1. Group 6 clusters

The synthesis of the trigonal-bipyramidal cluster $[Se_2Cr_3(CO)_{10}]^{2-}$ from $Cr(CO)_6$, SeO_2, and highly concentrated NaOH/MeOH solutions is described. Treatment of this novel selenium-capped cluster with $Mo(CO)_6$ in acetone furnishes the mixed-metal cluster $[Se_2Cr_2Mo(CO)_{10}]^{2-}$. The solid-state structures of each cluster were established by X-ray crystallography [5]. The reaction of $[(OC)_4Mo(\mu\text{-}Cl)_3Mo(CO)_3(SnCl_3)]$ with diphenylacetylene, after exposure to moist air, gives the oxo-capped cluster $Mo_3(\mu_3\text{-}O)(\mu_3\text{-}Cl)(\mu_2\text{-}Cl)(\mu_2\text{-}OH)_2(O)(\eta^2\text{-}PhC{\equiv}CPh)_5$, whose X-ray structure confirms the triangular array of molybdenum atoms. The mixed-valence Mo_2(II)Mo(IV) core is discussed relative to other molybdenum systems [6]. $Cp^*Mo(CO)_3Cl$ reacts with K_3AsS_3 to give several dimolybdenum complexes, of which $Cp^*_2Mo_2(CO)_2As_2S_4$ has been shown to undergo reaction with $Cr(CO)_5(THF)$ to furnish $[Cp^*_2Mo_2(CO)_2As_2S_4][Cr(CO)_5]_2$. The molecular structure of this Mo_2Cr_2 cluster reveals the presence of two AsS_2 ligands that bridge the two Mo atoms in a pseudoallylic manner. Each AsS_2 ligand acts as a seven-electron-donor group [7]. The preparation and magnetic properties of the cubane clusters $[CpCr(\mu_3\text{-}O)]_4(tcnq)$ and $[CpCr(\mu_3\text{-}O)]_4[BF_4]$ (where Cp = Cp, Cp*, MeCp) have been described. The redox properties of the starting clusters $[CpCr(\mu_3\text{-}O)]_4$ have been examined by differential pulse and cyclic voltammetric techniques. The X-ray structural data are discussed with respect to the Cr–Cr, Cr–O, and Cr–Cp bond distances of the clusters as a function of the oxidation state. The magnetic data for $[Cp^*Cr(\mu_3\text{-}O)]_4[tcnq]$ reveal that electronic coupling occurs between an unpaired electron on $[Cp^*Cr(\mu_3\text{-}O)]_4^+$ and one electron on $[tcnq]^-$ at temperatures below 110 K [8].

2.2. Group 7 clusters

Thermolysis of $Mn_2(CO)_{10}$ with $Cp_2Mo(SPh)_2$ yields the incomplete cubane cluster $[Mn_3(CO)_9(\mu\text{-}SPh)_4][Cp_2Mo(CO)(H)]$ in moderate yield. X-ray analysis reveals that the $[Cp_2Mo(CO)(H)]^+$ moiety is directed inward towards the vacant site of the cubane core. The solution spectroscopic data and plausible reaction mechanisms are discussed [9]. The reaction of $[Mn_3(\mu\text{-}H)(CO)_{12}]^{2-}$ with AuCl-terminated carbosilane dendrimers has been explored [10]. Treatment of $Re_3(\mu\text{-}H)_3(CO)_{11}(MeCN)$ with C_{60} in refluxing chlorobenzene gives $Re_3(\mu\text{-}H)_3(CO)_9(\mu_3\text{-}\eta^2,\eta^2,\eta^2\text{-}C_{60})$, which upon reaction with Me_3NO in the presence of PPh_3 gives $Re_3(\mu\text{-}H)_3(CO)_8(PPh_3)(\mu_3\text{-}\eta^2,\eta^2,\eta^2\text{-}C_{60})$. The nonacarbonyl cluster reacts with benzyl isocyanide at room temperature to afford the corresponding ligand substituted product. All three of these clusters have been fully characterized in solution and by X-ray analysis in the case of $Re_3(\mu\text{-}H)_3(CO)_8(CNCH_2Ph)(\mu_3\text{-}\eta^2,\eta^2,\eta^2\text{-}C_{60})$, whose X-ray structure is shown in Fig. 1. Cyclic voltammetric data recorded in chlorobenzene suggest that a C_{60}-mediated electron transfer to the Re_3 core is quite facile in comparison to the redox data reported for other C_{60}-substituted clusters [11].

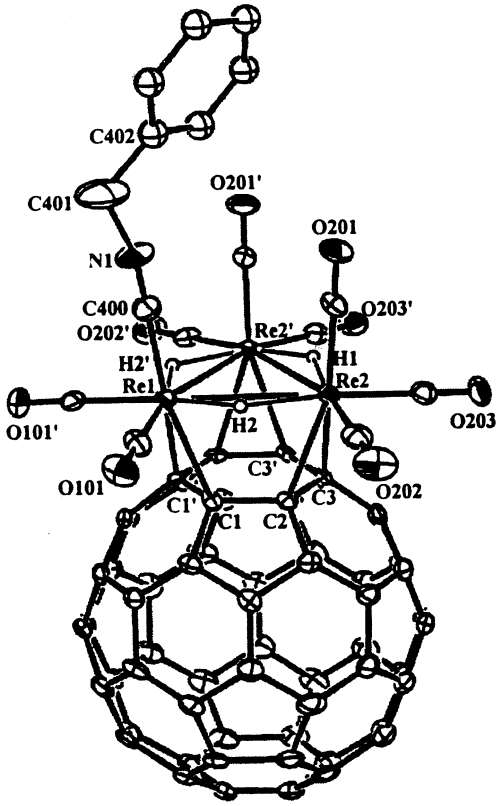

Fig. 1. X-Ray structure of $Re_3(\mu\text{-}H)_3(CO)_8(CNCH_2Ph)(\mu_3\text{-}\eta^2,\eta^2,\eta^2\text{-}C_{60})$. Reprinted with permission from Organometallics. Copyright 2001 American Chemical Society.

Physisorbed $[Re_2(CO)_6(\mu\text{-}OH)_3][K]$ on a silica surface has been achieved when $[Re(CO)_3OH]_4$ and K_2CO_3 are allowed to react with a slurry of SiO_2 [12]. The complex $Mn_2(CO)_6(\mu\text{-}CO)(\mu\text{-}S_2)$ reacts with PMe_2Ph at room temperature to afford $Mn_4S_4(CO)_{15}(PMe_2Ph)_2$ in moderate yield [13]. The reactivity of $Re_2(CO)_8(THF)_2$ with carbonyl-rhenates possessing two terminal hydrides has been investigated. Use of $[Re_2H_2(\mu\text{-}H)(CO)_8]^-$ and the bis(THF) adduct furnishes the tetrarhenium cluster $[Re_4(\mu\text{-}H)_3(CO)_{16}]^-$, whose X-ray structure exhibits a puckered-square metal core. This anionic Re_4 cluster is readily protonated to give $Re_4(\mu\text{-}H)_4(CO)_{16}$; however, the reaction cannot be reversed by treatment with bases. Photochemical activation of $Re_4(\mu\text{-}H)_4(CO)_{16}$ gives the unsaturated dimer $Re_2(\mu\text{-}H)_2(CO)_8$. The X-ray data are discussed relative to the results obtained from density functional calculations [14].

2.3. Group 8 clusters

A study on the kinetics of the radical-chain process in the reaction between $Fe_3(CO)_{12}$ and $[Et_4N][SEt]$ has appeared. EPR data show the existence of $[Fe_3(CO)_{12}]^{-\bullet}$ and $[Fe_3(CO)_{11}]^{-\bullet}$ via stopped-flow methodology. Data are presented that support an inverse kinetic scheme, that is further substantiated by computer modeling of the time–concentration dependence of both radical anions [15]. The reaction of $Fe_3(CO)_{12}$ with 1-ethynylcyclohexanol gives several dinuclear species along with $Fe_3(CO)_9(\mu\text{-}CO)[\mu_3\text{-}\eta^2\text{-}1,2\text{-}HC{\equiv}C(C_6H_{10}OH)]$, $Fe_3(CO)_9(\mu\text{-}CO)[\mu_3\text{-}\eta^2\text{-}1,2\text{-}C{=}C(C_6H_{10})]$, and $Fe_3(CO)_7[\mu_3\text{-}\eta^7\text{-}(C_6H_{10}OH)CCHCHC(C_6H_9)]$. The latter cluster, whose molecular structure was determined by X-ray crystallography, contains a parallel alkynol ligand, an allenylidene moiety, and a metallocyclic ligand. The solution data from IR and NMR spectroscopic studies are included, and plausible reaction pathways leading to the formation of these Fe_3 clusters are presented [16]. A paper describing the preparation of resin-bound amine N-oxides and their use in synthetic carbonyl cluster chemistry has appeared. The resin-bound amine N-oxides were employed in the decarbonylation of $Ru_3(CO)_{12}$ and $Os_3(CO)_{12}$ to afford the corresponding mono- and bis-acetonitrile derivatives [17]. The preparation of barium-promoted oxide-supported ruthenium catalysts from $Ru_3(CO)_{12}$ and their use in the low-energy, low-pressure synthesis of ammonia have been described. Details associated with the catalytic process and the effect of the promoter on the turnover and selectivity for the reaction are discussed [18]. The dehydrogenative silylation of aryloxazolines with hydrosilanes is readily catalyzed by $Ru_3(CO)_{12}$. The oxazoline group is shown to direct the silylation in an *ortho* fashion relative to the heterocyclic moiety. The coupling reaction is operative in the presence of electron-donating and electron-withdrawing groups [19]. The activation of the sp^3 C–H bond adjacent to the nitrogen atom in *N*-2-pyridynyl alkylamines, followed by the coupling with an alkene, has been achieved by using $Ru_3(CO)_{12}$ as a catalyst. The presence of a nitrogen directing atom is interpreted in terms of a mechanism involving nitrogen coordination to the ruthenium catalyst. The critical role played by the reaction solvent and reaction schemes are discussed [20]. The regioselective C–C bond formation between ethylene and α-naphthylcarbaldimes has been demonstrated when $Ru_3(CO)_{12}$ is used as a catalyst precursor. When the reaction is monitored by NMR spectroscopy evidence is found for the involvement of a dinuclear ruthenium carbonyl complex. The X-ray structure of one Ru_2 intermediate accompanies this report [21]. The $Ru_3(CO)_{12}$-catalyzed carbonylation of piperidine has been examined by in-situ high-pressure IR spectroscopy. IR data confirm the presence of $Ru(CO)_5$ as the major organometallic species under autogeneous catalysis. Despite the fact that the carbonylation is slow, the reaction is very clean, giving the *N*-formyl amine as the predominant product. The effect of the CO pressure on the reaction and a plausible mechanism are described [22]. A report on the intramolecular hydroamination of aminoalkynes using $Ru_3(CO)_{12}$ has appeared. The reaction is highly regioselective, affording five-, six-, and seven-membered nitrogen heterocycles and indoles through nitrogen attachment to an internal alkyne carbon atom [23]. The first alkyl-group transfer from trialkylamines to the α-C atom of ketones has been reported. Use of $Ru_3(CO)_{12}$ as a catalyst precursor gives a low conversion to the homologated ketone [24]. $Ru_3(CO)_{12}$ has been employed as a catalyst for the synthesis of spiro[pyrrolidin-2-one] derivatives by a [2+2+1] cycloaddition of ketimines, CO, and ethylene [25]. Nitrobenzene reduction has been investigated under water–gas-shift conditions by catalyst systems composed of $Ru_3(CO)_{12}$ and chelating diimines. The chemoselectivity for nitro group reduction relative to the alkene and keto groups is reported to be high [26]. The hydrogenation and isomerization of 1-hexene with $Ru_3(CO)_{12}$ and $Ru_3(CO)_9(PPh_3)_3$ have been studied in the presence and absence of H_2. IR examination of the reaction with the latter cluster and with $Ru_3(CO)_{12}/PPh_3$ reveals the presence of $H_4Ru_4(CO)_{12}$ and $H_4Ru_4(CO)_{12-n}(PPh_3)_n$ (where $n = 1$–4) [27]. $Os_3(CO)_{12}$ and 2,2,6,6-tetramethyl-3,5-heptanedionate react at 180 °C in an autoclave to give the metal chain complex $[Os_2(CO)_5(L)_2]_2$ and $Os_4(\mu\text{-}H)(\mu\text{-}CO_2)(L)(CO)_{13}$ in low yields. Both compounds were characterized in solution and by X-ray diffraction analysis in the case of the latter cluster. The presence of a unique CO_2 ligand in the X-ray structure is discussed [28]. Treatment of $Ru_3(CO)_{12}$ with $C_5Me_4HMe_2GeGeMe_2C_5Me_4H$ in boiling decalin furnishes the trigonal-bipyramidal compound $[(\mu_3\text{-}Ge)\{Ru(CO)_2(\eta^5\text{-}C_5Me_4H)\}]_2Ru_3(CO)_9$,

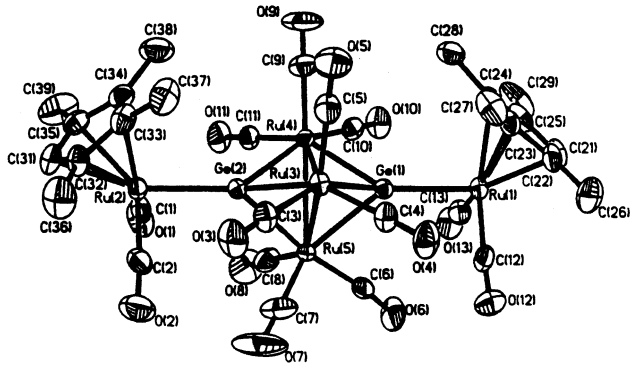

Fig. 2. X-Ray structure of $[(\mu_3\text{-Ge})\{Ru(CO)_2(\eta^5\text{-}C_5Me_4H)\}]_2Ru_3(CO)_9$. Reprinted with permission from Organometallics. Copyright 2001 American Chemical Society.

whose the X-ray structure is shown in Fig. 2, and the diruthenium complex $(Me_2Ge)(\eta^5\text{-}C_5Me_4H)Ru_2(CO)_6$. Use of the germanium compound $C_5H_4Me_2GeGeMe_2C_5H_4$ with $Ru_3(CO)_{12}$ gives three different bimetallic compounds [29].

The thermolysis of commo-[1-(Cp*Ru)(μ-H)B_4H_9]$_2$Ru in refluxing benzene provides $[(Cp^*Ru)_2(\eta^6\text{-}C_6H_6)RuB_7H_7]$. The hypoelectronic triruthenaborane cluster has been characterized in solution by ^{11}B-NMR spectroscopy and by X-ray crystallography. The polyhedral distortion of this cluster from the expected canonical shape is discussed relative to borane bonding models [30]. The deprotonation chemistry of ferraborane clusters and their relative acidities have been investigated. The cluster compounds subjected to examination include $HFe_4(CO)_{12}BH_2$, $HFe_3(CO)_9BH_4$, and $HFe_3(CO)_{10}BH_2$ [31]. The reaction between $CpOs(PPh_3)_2Br$ and $Os_3(\mu_3\text{-}Me_3SiC_2C{\equiv}CSiMe_3)(CO)_9$ in methanol solvent affords $Os_3(\mu_3\text{-}Me_3SiC_2C{\equiv}CSiMe_3)(\mu\text{-}OMe)_2(CO)_9$. The X-ray structure of this 52-electron cluster exhibits an opened core, where the two non-bonded Os–Os vectors are each bridged by one OMe group [32]. A report on the reactivity of multi-site bound allenylidene ligands towards alkynes and silica gel has appeared. Heating the allenylidene cluster $Ru_3(CO)_9(\mu\text{-}CO)(\mu_3\text{-}C{=}C{=}CPh_2)$ with RC_2R (where R = Me, Ph) furnishes the clusters $Ru_3(CO)_9[\mu_3\text{-}C(R)C(R)C_2CPh_2]$ and $Ru_4(CO)_{12}[\mu_4\text{-}C(Ph)C(Ph)CCCPh_2]$. X-ray diffraction analysis of the latter cluster confirms the presence of the C_5 ligand that is formed through C–C bond formation with the α-carbon of the allenylidene ligand. Treatment of the starting allenylidene cluster with silica gel at room temperature gives the acetylide cluster $Ru_3(CO)_9(\mu\text{-}H)[\mu_3\text{-}C{\equiv}CC(Ph)_2OH]$, while $Ru_3(CO)_9(\mu\text{-}CO)[\mu_3\text{-}C{=}C{=}C(Ph)(Me)]$ reacts with silica gel to afford the ene-yne-substituted cluster $Ru_3(CO)_9(\mu\text{-}H)[\mu_3\text{-}C{\equiv}CC(Ph){=}CH_2]$. Mechanisms that account for these transformations are presented and discussed [33]. The reactivity of $Os_3(CO)_{10}(MeCN)_2$ with symmetric diynes, followed by the reaction of the resulting adduct with $Co_2(CO)_8$, has been studied. The reaction between MeC_2C_2Me and $Os_3(CO)_{10}(MeCN)_2$ leads to the new clusters $Os_3(CO)_9(\mu\text{-}CO)(\mu_3\text{-}\eta^2{:}\mu_3\text{-}\eta^1{:}\eta^1{:}\eta^3\text{-}MeC_2C_2MeOC_5Me_2)Os_3(\mu\text{-}CO)(CO)_9$, $Os_3(CO)_9[\mu_3\text{-}\eta^4\text{-}\{(MeC_2)C_2(Me)\}CO\{(Me)C_2(C_2Me)\}]$, and $Os_3(CO)_9[\mu_3\text{-}\eta^4\text{-}\{(MeC_2)C_2(Me)\}CO\{(MeC_2)C_2(Me)\}]$, along with the expected product $Os_3(CO)_9(\mu\text{-}CO)(\mu_3\text{-}\eta^2\text{-}MeC_2C_2Me)$. X-ray crystallography reveals that the first cluster is composed of two linked Os_3 clusters that are joined by an unsaturated five-membered metallocycloether ring, while the second product contains an alkyne-functionalized metallocyclohexadieneone ring. The reaction of $Os_3(CO)_9(\mu\text{-}CO)(\mu_3\text{-}\eta^2\text{-}PhC_2C_2Ph)$ and aforementioned osmium clusters with $Co_2(CO)_8$ has been studied. The six new clusters isolated have been fully characterized in solution and by X-ray crystallography. The CO substitution chemistry of several cluster systems has been examined and the results discussed [34]. The molecular structures and electrocommunication between ferrocenyl groups of new triosmium cluster have been described. 1,8-Bis(ferrocenyl)octatetrayne has been allowed to react with $Os_3(CO)_{11}(MeCN)$ to give $Os_3(CO)_{10}(\mu_3\text{-}\eta^2\text{-}FcC_2C{\equiv}CC{\equiv}CC{\equiv}CFc)$, $Os_3(CO)_{10}(\mu_3\text{-}\eta^2\text{-}FcC{\equiv}CC_2C{\equiv}CC{\equiv}CFc)$, $Os_3(CO)_{11}(\mu_3\text{-}\eta^4\text{-}FcC_4C{\equiv}CC{\equiv}CFc)$, and $Os_6(CO)_{21}(FcC_2C_3COCC{\equiv}CFc)$. The first two clusters are also obtained in good yields when $Os_3(CO)_{10}(MeCN)_2$ was used as a starting material, along with the hexaosmium cluster $Os_6(CO)_{20}(\mu_6\text{-}\eta^4\text{-}FcC{\equiv}C_2C{\equiv}CC_2Fc)$. All five clusters were characterized in solution by IR and NMR spectroscopy, and their solid-state structures were determined by X-ray crystallography. The redox behavior of these clusters has been investigated by cyclic and differential pulse methodologies [35]. The reactivity of four different ruthenium clusters with alkynes has been studied. The four clusters isolated and structurally characterized include $Ru_3(\mu_3\text{-}PhC_2C{=}CHPh)(\mu\text{-}OH)(CO)_9$, $Ru_3[\mu_3\text{-}C(OCH_2CH{=}CH_2)CHCCPh_2OC(O)](\mu\text{-}dppm)(\mu\text{-}CO)(CO)_6$, $Ru_4(\mu_4\text{-}PhCHC_2CHPh)(CO)_{12}$, and $Ru_4(\mu_4\text{-}CHCCH_2CHPMe_3)(CO)_{10}(PMe_3)$ [36].

A review discussing the coordination and the transformations of arene ligands at transition metal carbonyl clusters has appeared. The synthetic pathways, reactivity, and catalytic behavior of these benzene-substituted clusters are discussed [37]. A report on the ligand-induced conversion of Π to σ C_{60}-cluster compounds has been published. Thermolysis of $Os_3(CO)_8(CNR)(\mu_3\text{-}\eta^2,\eta^2,\eta^2\text{-}C_{60})$ with excess benzyl isocyanide at 80 °C leads to two compounds formulated as $Os_3(CO)_8(CNR)_2(C_{60})$. The original $\mu_3\text{-}\eta^2,\eta^2,\eta^2$ (Π) C_{60} coordination to the Os_3 frame changes to a $\mu_3\text{-}\eta^1,\eta^1,\eta^1$ (σ) coordination mode, as demonstrated by X-ray crystallography [38].

Glycols react with $Os_3(\mu\text{-}H)(CO)_{10}(\mu\text{-}OH)$ to furnish clusters having the general formula $Os_3(\mu\text{-}H)(CO)_{10}(\mu\text{-}$

O–OH). The reactivity of the glycol-coordinated clusters has also been examined. $Os_3(\mu\text{-}H)(CO)_{10}(\mu\text{-}OCH_2\text{-}CH_2OH)$ undergoes esterification with benzoyl chloride to give $Os_3(\mu\text{-}H)(CO)_{10}[\mu\text{-}OCH_2CH_2OC(O)Ph]$, along with $Os_3(\mu\text{-}H)(CO)_{10}(\mu\text{-}OCH_2CHO)$. The allylation chemistry of this latter cluster and its reactivity towards PhMgBr are reported. The solution spectroscopic data and the diffraction data from five clusters are discussed [39]. 18β-glycyrrhetinic acid (18β-GA) has been allowed to react with $Os_3(CO)_{10}(MeCN)_2$ and $Ru_3(CO)_{12}$ to give $Os_3(\mu\text{-}H)(\mu\text{-}O_2C\text{-}C_{29}H_{45}O_2)(CO)_{10}$ and $Ru_2(\mu\text{-}O_2C\text{-}C_{29}H_{45}O_2)_2(CO)_4(THF)_2$, respectively. X-ray data confirm that the 18β-GA residue is coordinated to the Os_3 frame by the carboxylate moiety, with the oleanic organic moiety being oriented exo relative to the plane defined by the three osmium atoms [40]. The ring-opening polymerization of norbornene to give high molecular weight poly(1,3-cyclopentylene-vinylene) in high yield is catalyzed by $(\mu\text{-}H)_2Os_3(CO)_{10}$. A reaction mechanism involving a dimetallacyclopentene intermediate is presented, and the all *cis* structure of the polymer is supported by IR and ^{13}C-NMR data [41]. The chemical and thermal behavior of the clusters $Os_3(CO)_{10}(\mu\text{-}H)(\mu\text{-}OSiR_2R')$ (where R = Et, Ph; R′ = Et, Ph, OH, $OSiPh_2OH$), which serve as molecular models for silica-anchored $Os_3(CO)_{10}(\mu\text{-}H)(\mu\text{-}OSi\equiv)$, has been investigated. These models have the ability to function as springboards for the understanding and molecular clarification for the reactivity of organometallic species on the surface of silica [42]. Molecular H_2 exchange in $(\mu\text{-}H)_2Os_3(CO)_{10}$ has been investigated by H_2/D_2 isotopic exchange studies, and *para*-H_2 effects on the ^{1}H-NMR spectrum of the cluster have been studied. Of the two exchange pathways observed, the most efficient exchange path involves an associative process with the species $(\mu\text{-}X_2)(H)(\mu\text{-}H)Os_3(CO)_{10}$ (where X_2 = D_2 or *para*-H_2), which undergoes XH elimination. The dissociative path is also observed, and the unsaturated $Os_3(CO)_{10}$ cluster is shown to rapidly add X_2 to give the asymmetrical cluster $X(\mu\text{-}X)Os_3(CO)_{10}$(solvent) [43]. The reactivity of several substituted diynes with $H_2Os_3(CO)_{10}$ has been studied. The X-ray structures of $HOs_3(CO)_{10}[\mu\text{-}\eta^1\text{:}\eta^1\text{-}MeCC{=}CC(H){=}C(H)NPh]$ (Fig. 3) and four other clusters accompany this report. Diyne cyclization chemistry and hydride transfer reactivity are discussed, along with plausible reactions mechanisms [44].

The interpretation of the ν(M–M) Raman spectra of twenty doubly bridged triosmium clusters via a modified plastic cluster model has been presented. This model incorporates the mass of all of the ligands in the normal co-ordinate analysis. The clusters examined possess the general form $Os_3(X)(Y)(CO)_{10}$ [45]. The catalytic hydrogenation of arenes under biphasic conditions employing $[(\eta^6\text{-}C_6Me_6)_2(\eta^6\text{-}C_6H_6)Ru_3(\mu_3\text{-}H)_3(\mu_3\text{-}O)]^+$ is reported to give cyclohexanes. There is a high substrate selectivity observed, with ethylbenzene hydrogenation exhibiting extremely high activity. The isolation and structural characterization of $[(\eta^6\text{-}C_6Me_6)_2(\eta^6\text{-}C_6H_6)Ru_3(\mu_2\text{-}H)_2(\mu_2\text{-}OH)(\mu_3\text{-}O)]^+$ are presented, and the hydrogenation turnover frequencies are tabulated and discussed relative to other hydrogenation systems [46]. Carbonylation of $Ru_3(CO)_6(\mu\text{-}CO)(\mu_3\text{-}\eta^5\text{:}\eta^3\text{:}\eta^3\text{-}C_{10}H_8)$ affords the metastable cluster $Ru_3(CO)_8(\mu_3\text{-}\eta^5\text{:}\eta^2\text{:}\eta^1\text{-}C_{10}H_8)$, which upon additional CO capture gives $Ru_2(CO)_5(\mu_2\text{-}\eta^5\text{:}\eta^3\text{-}C_{10}H_8)$. These complexes were characterized in solution by IR and NMR (^{1}H-COSY, -HMQC, and two-dimensional (2-D) methods) spectroscopies, and by X-ray diffraction analysis in the case of the Ru_2 complex. The bonding changes associated with the azulene ligand are outlined in the proposed reaction mechanism [47]. The μ_3-borylene complexes $(Cp^*Ru)_3(\mu\text{-}H)_3(\mu_3\text{-}BX)$ (where X = H, CN) have been obtained from the reaction of $[(Cp^*Ru)_3(\mu\text{-}H)_6][BF_4]$ with $NaBH_3X$. Treatment of the μ_3-borylene clusters with ROH affords the corresponding μ_3-BOR analogue. Sulfur–carbon bond cleavage in benzothiophene to afford the μ_3-thioruthenacyclohexadiene cluster $(Cp^*Ru)_3(\mu\text{-}H)(\mu_3\text{-}BH)(SC_8H_6)$ is observed when the μ_3-BH cluster is treated with the aforementioned heterocycle. Solution NMR data and two X-ray structures accompany this report [48]. Carbon–carbon double bond cleavage in 1,1-disubstituted alkenes has been demonstrated at a triruthenium cluster. $(Cp^*Ru)_3(\mu\text{-}H)_3(\mu_3\text{-}H)_2$ undergoes reaction with a variety of 1,1-disubstituted alkenes to furnish clusters having the general formula $(Cp^*Ru)_3(\mu_3\text{-alkyne})(\mu_3\text{-methylidyne})$ [49].

Treatment of $Ru_3(\mu\text{-}H)(\mu\text{-}\eta^2\text{-}Me_2pz)(CO)_{10}$ with 2,4-hexadiyne gives the tetraruthenium ynenyl cluster $Ru_4(\mu\text{-}\eta^2\text{-}Me_2pz)(\mu_4\text{-}\eta^4\text{-}MeCH{=}C{-}C{\equiv}CMe)(\mu\text{-}CO)\text{-}(CO)_{10}$. This 64-electron cluster exhibits an unusual broken-wing butterfly structure, where the 7-electron hex-2-yn-4-en-4-yl ligand bridges all four ruthenium centers [50]. The isomeric clusters $Os_3(CO)_9(\mu\text{-}py)(\mu_3,\eta^3\text{-}CCFcCCHFc)$ and $Os_3(CO)_9(\mu\text{-}py)(\mu_3,\eta^2\text{-}CCFcCCHFc)$ have been isolated as the major products from the reaction between $Os_3(CO)_{10}(\mu\text{-}\eta^2\text{-}py)(\mu\text{-}H)$, 1,4-bis(ferrocenyl)butadiyne, and Me_3NO. The presence of a triply bridging 1,3-bisferrocenylallylcarbyne ligand in each open triosmium cluster was verified by X-ray crystallography. The redox chemistry of both products was investigated by differential pulse voltammetry [51]. The formation of a diynedienyl ligand via coupling of hexa-2,4-diyne and hex-2-yn-4-en-4-yl ligands on a triruthenium cluster has been demonstrated. $Ru_3(\mu\text{-}H)(\mu_3\text{-}\eta^2\text{-ampy})(CO)_9$ reacts with the diyne ligand to produce ultimately $Ru_3(\mu\text{-}H)(\mu_3\text{-}\eta^2\text{-ampy})[\mu\text{-}\eta^5\text{-}MeC{\equiv}CC(=CHMe)CMe{=}CC{\equiv}CMe](\mu\text{-}CO)(CO)_5$, whose X-ray structure is shown below. The role played by $Ru_3(\mu_3\text{-}\eta^2\text{-ampy})(\mu\text{-}\eta^3\text{-}MeCH{=}CC{\equiv}CMe)(\mu\text{-}CO)_2\text{-}$

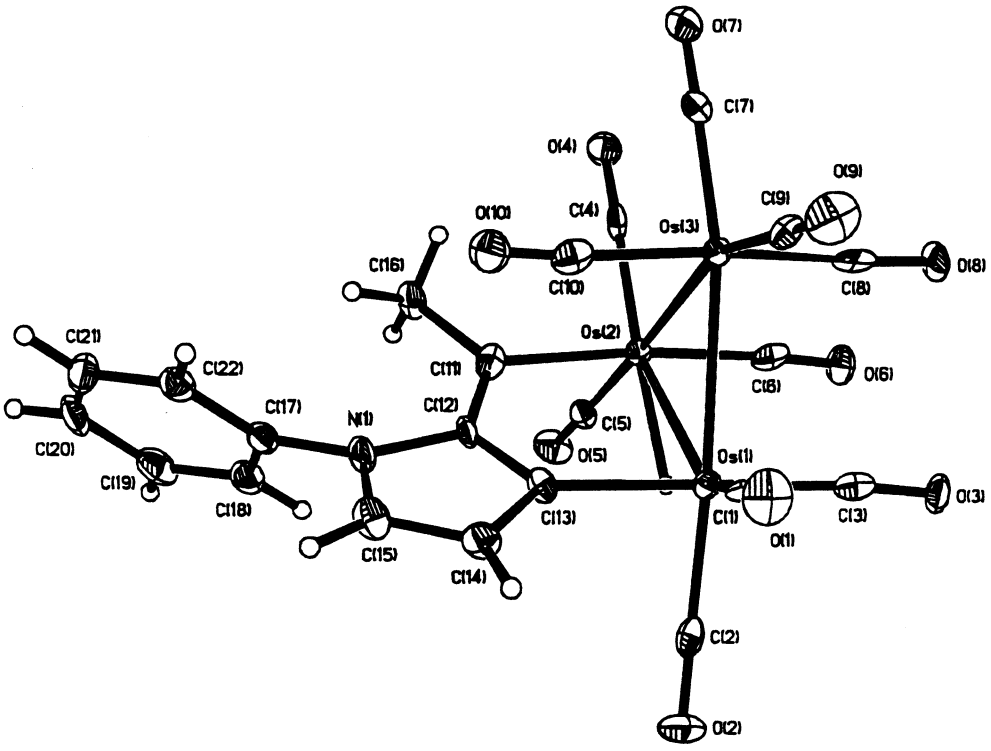

Fig. 3. X-Ray structure of $HOs_3(CO)_{10}[\mu\text{-}\eta^1\text{:}\eta^1\text{-MeCC=CC(H)=C(H)NPh}]$. Reprinted with permission from Organometallics. Copyright 2001 American Chemical Society.

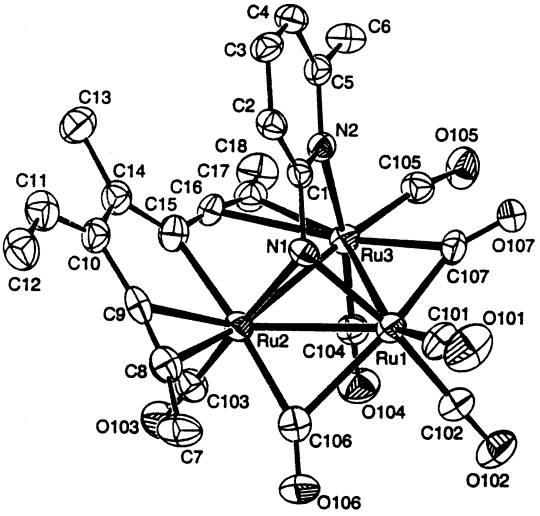

Fig. 4. X-Ray structure of $Ru_3(\mu\text{-H})(\mu_3\text{-}\eta^2\text{-ampy})[\mu\text{-}\eta^5\text{-MeC}\equiv\text{CC}(=\text{CHMe})\text{CMe}=\text{CC}\equiv\text{CMe}](\mu\text{-CO})(\text{CO})_5$. Reprinted with permission from Organometallics. Copyright 2001 American Chemical Society.

$(CO)_6$ in the production of the final cluster product is discussed (Fig. 4) [52].

The sulfoximido-substituted clusters $Ru_3(CO)_9(\mu_2\text{-H})[\mu_3\text{-NS(O)MePh}]$, $Ru_3(CO)_{10}(\mu_2\text{-H})[\mu_3\text{-NS(O)MePh}]$, $Ru_3(CO)_8(\mu_3\text{-}\eta^2\text{-CPhCHBu})[\mu_3\text{-NS(O)MePh}]$, $Ru_3(CO)_9(\mu_3\text{-}\eta^2\text{-PhCCCCHPh})[\mu_2\text{-NS(O)MePh}]$, and $Ru_3(CO)_7(\mu_2\text{-CO})(\mu_3\text{-}\eta^2\text{-PhCCCCHPh})[\mu_3\text{-NS(O)MePh}]$ have been investigated by extended Hückel and DFT calculations. The MO data are used in the analysis of cluster bonding and verification of the electron-donor contribution of the sulfoximido ligands. The μ_3-sulfoximido moiety is shown to act as a three-orbital/5e-system that is isolobal to the RN^- ligand. The same ligand functions as two-orbital/3e-donor when it adopts a μ_2 coordination mode. The adherence of these clusters to electron-precise and PSEP bonding theories is discussed [53]. New clusters containing sulfur, ynyl, and diynyl ligands have been synthesized and subjected to X-ray analysis. $Ru_3(CO)_{12}$ has been allowed to react with $S(C\equiv CSiMe_3)_2$ to initially afford $Ru_3(CO)_9(\mu\text{-}\eta^2\text{-SC}\equiv CSiMe_3)(\mu_3\text{-}\eta^2\text{-C}\equiv CSiMe_3)$, which upon thermolysis leads to S–C bond cleavage and C–C bond coupling of the acetylide groups to furnish $Ru_3(CO)_9(\mu_3\text{-S})[\mu_3\text{-}\eta^2\text{-C(SiMe}_3)\text{C}(C\equiv CSiMe_3)]$, $Ru_4(CO)_{12}(\mu_4\text{-S})(\mu\text{-}\eta^2\text{-C}\equiv CSiMe_3)_2$, and $Ru_4(CO)_9(\mu\text{-CO})_2(\mu_4\text{-S})[\mu_4\text{-}\eta_2\text{-C(SiMe}_3)\text{C}(C\equiv CSiMe_3)]$. Pathways for cluster reactivity are discussed [54]. The thioethers R_2S (where R = Et, ^{n}Pr) and MeS^tBu react with $Os_3(CO)_{11}(MeCN)$ to give $Os_3(CO)_{11}(L)$, in which the thioether ligand is situated in an equatorial site. The orthometallated clusters $Os_3(\mu\text{-H})(CO)_{10}(\mu\text{-}\eta^2\text{-}C_6H_4SR)$ and $Os_3(\mu\text{-H})(CO)_9(\mu_3\text{-}C_6H_4SPh)$ were obtained as the major products from the reaction of $Os_3(CO)_{10}(MeCN)_2$ with the thioethers Ph_2S and MeSPh. No discernable products are observed in the thermal reaction of $Os_3(\mu\text{-H})_2(CO)_{10}$ and other thioethers; however, use of Me_3NO does afford clusters having the formula $Os_3(CO)_9(\mu\text{-H})_2$(thioether). Included

in this report are the X-ray structures of $Os_3(CO)_{11}(L)$ [where $L = Et_2S$, Pr_2S, $S(CH_2)_5$] and $Os_3(CO)_9(\mu\text{-}H)(\mu\text{-}X)(SMe^tBu)$ (where $X = H$, OH) [55]. New sulfido-capped ruthenium clusters containing kinetically labile MeCN ligands have been prepared. Irradiation of $[(cymene)_3Ru_3S_2]^{2+}$ in MeCN affords $[(cymene)_2(MeCN)_3Ru_3S_2]^{2+}$ as the sole product. The reactivity of this cluster towards PPh_3 and 1,4,7-trithiacyclononane has been explored, and the elongated Ru–Ru bonds in $[(cymene)_2(MeCN)_{3-x}(PPh_3)_xRu_3S_2]^{2+}$ (where $x = 1$, 2) and $[(cymene)_2(9S3)Ru_3S_2]^{2+}$ have been confirmed by X-ray crystallography. The redox chemistry of these new clusters has been studied by cyclic voltammetry, and the pentaruthenium cluster $[(cymene)_4Ru_5S_4]^{2+}$, which was isolated from the prolonged irradiation of the starting cluster in the presence of MeCN, has been structurally characterized and found to exhibit a bow-tie structure (Fig. 5) [56].

Ruthenium and platinum clusters have been prepared and examined for DNA binding activity in MeOH/H_2O and H_2O solutions. The clusters examined include $[H_4Ru_4(C_6H_6)_4]^{2+}$, $Ru_3(CO)_9(PTA)_3$, $[Pt_3(dpmp)_2(XylNC)_2]^{2+}$, $[Pt_3(\mu_3\text{-}CO)(\mu\text{-}dppm)_3]^{2+}$, and $H_4Ru_4(CO)_{12}$, of which the former two clusters were found to be the most effective in cross linking and intercalation of DNA, respectively, [57]. The new phosphine ligand $Ph_2PC_6H_4\text{-}4\text{-}C{\equiv}CSiMe_3$ has been employed in the synthesis of $Ru_3(CO)_9(Ph_2PC_6H_4\text{-}4\text{-}C{\equiv}CSiMe_3)_3$, and which upon treatment with carbonate or fluoride furnishes $Ru_3(CO)_9(Ph_2PC_6H_4\text{-}4\text{-}C{\equiv}CH)_3$. This latter cluster undergoes reaction with $[CpRu(PPh_3)_2(MeCN)]^+$ to give $Ru_3(CO)_9[(Ph_2PC_6H_4\text{-}4\text{-}C{\equiv}C)Ru(PPh_3)_2Cp]$. The redox chemistry of these clusters and data from the X-ray structural studies are discussed [58]. Facile cluster coupling reactivity via a selenium atom has been demonstrated by using Ph_3PSe. Treatment of $Os_3(CO)_{11}(MeCN)$ with Ph_3PSe at room temperature gives the known clusters $Os_3(\mu_3\text{-}Se)_2(CO)_9$ and $Os_3(CO)_{11}(PPh_3)$, and the new cluster $Os_3(\mu_3\text{-}Se)(CO)_9(PPh_3)$, while use of $Os_3(CO)_{10}(MeCN)_2$ gives only the first two known cluster products. The hydrido cluster $Os_3(\mu\text{-}H)_2(CO)_{10}$ reacts with Ph_3PSe to furnish the new cluster products $Os_3(\mu_3\text{-}Se)(\mu\text{-}H)_2(CO)_8(PPh_3)$ and $Os_6(\mu_3\text{-}Se)(H)(\mu\text{-}H)_3(CO)_{18}(PPh_3)_2$. The X-ray structure of the Os_6 cluster reveals the presence of a naked μ_3-Se atom that bridges an $Os_3(\mu\text{-}H)(CO)_{10}$ moiety and an $Os_3(H)(\mu\text{-}H)_2(CO)_8(PPh_3)_2$ moiety [59]. 1,2,3-Triphenyl-1,2,3-triphosphaindan has been allowed to react with the activated clusters $Os_3(CO)_{11}(MeCN)$ and $Os_3(CO)_{10}(MeCN)_2$. The phosphine ligand undergoes facile reaction with $Os_3(CO)_{11}(MeCN)$ at room temperature to give the mono-substituted cluster $Os_3(CO)_{11}[1\text{-}C_6H_4(PPh)_3]$ and the bridged bis-trinuclear cluster $[Os_3(CO)_{11}]_2[\mu\text{-}1,3\text{-}\eta^2\text{-}C_6H_4(PPh)_3]$. Carrying out the reaction at 100 °C gives the latter product along with the disubstituted bridged cluster $Os_3(CO)_{10}[\mu\text{-}1,3\text{-}\eta^2\text{-}C_6H_4(PPh)_3]$, while at 140 °C the linked pentaosmium cluster $Os_2(CO)_6[\mu_3\text{-}\eta^3\text{-}PPhC_6H_4(PPh)_2]Os_3(CO)_{11}$, whose X-ray structure reveals the presence of only two Os–Os bonds, and the triosmium cluster $Os_3(CO)_9[\mu_3\text{-}\eta^3\text{-}PPhC_6H_4(PPh)_2]$ are observed as the major products. Interconversion mechanisms and the VT ^{31}P-NMR data associated with these clusters are discussed [60]. Tris(2-furyl)phosphine reacts with $Ru_3(CO)_{12}$ at elevated temperatures to produce $Ru_2(CO)_6[\mu\text{-}P\{C(CH)_3O\}_2\{\mu\text{-}\eta^1,\eta^2\text{-}C(CH)_3O\}]$ as the major product and $Ru_3(CO)_{10}[P\{C(CH)_3O\}_3]$ as the minor product [61]. ^{31}P-EXSY spectroscopy has been employed in the study of $Ru_3(CO)_{10}(PMe_2Ph)_2$ and $Ru_3(CO)_{10}(PPh_3)_2$. Three different isomeric forms of each cluster were observed and their interconversion chemistry verified by EXSY and line shape analysis. Solvent participation and the calculated activation parameters indicate that P-ligand migration between ruthenium centers proceeds by a heterolytic Ru–Ru bond cleavage when the intermediates are stabilized by the solvent. These same clusters have also been investigated for their reactivity with para hydrogen. Hydrogen activation takes place at a 16-electron ruthenium center formed after Ru–Ru bond heterolysis, followed by CO loss and reformation of the Ru–Ru bond. Detailed exchange mechanisms are presented and discussed relative to the thermodynamic and kinetic data [62]. K-Selectride reacts with $[Ru_3(\mu\text{-}PPh_2)(CO)_9]_2(\mu_3{:}\mu_3\text{-}C_4)$, followed by acidification, to afford $[Ru_3H(\mu\text{-}PPh_2)(CO)_9]_2(\mu_3{:}\mu_3\text{-}C{=}CHCH{=}C)$. The X-ray structure of this product confirms the addition of hydrogen to each Ru_3 cluster and the C_4 bridging fragment. The osmium analogue exhibits similar reactivity. Treatment of the starting ruthenium cluster with dihydrogen furnishes the pentanuclear complex

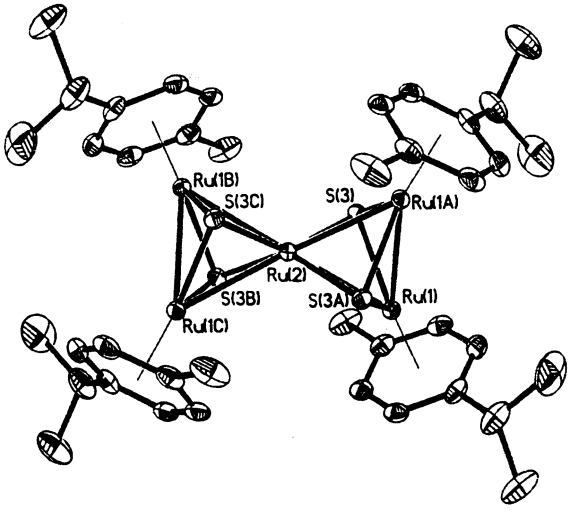

Fig. 5. X-Ray structure of $[(cymene)_4Ru_5S_4]^{2+}$. Reprinted with permission from Inorganic Chemistry. Copyright 2001 American Chemical Society.

$Ru_3[\mu_3{:}\mu\text{-}C_2C_2\{Ru(\mu\text{-}PPh_2)(CO)_6\}](\mu\text{-}PPh_2)(CO)_9$ through the formal cleavage of a $Ru(CO)_3$ fragment from the parent cluster [63]. CO ligand fluxionality and the X-ray structures of $Fe_3(CO)_{10}L_2$ [where L = dppm, $(Ph_2P)_2NH$, $\{(EtO)_2P\}_2O$] and $Fe_3CO)_9$(dppm)-[$P(OMe)_3$] have been the subject of a detailed investigation related to the exchange pathways available to P-substituted clusters. The dynamic behavior of these clusters is strongly influenced by the nature of the ancillary phosphine ligand(s), and the exchange pathways are discussed relative to the Mann concerted bridge-opening bridge-closing mechanism and the Johnson libration mechanism [64]. New phosphido–selenido clusters have been synthesized from Ph_2[5-(2-pyridyl)-2-thienyl]PSe and its reaction with $Ru_3(CO)_{12}$. The clusters $Ru_3(\mu_3\text{-}Se)_2(CO)_7$[P{5-(2-pyridyl)-2-thienyl}-Ph_2]$_2$ and $Ru_3(\mu_3\text{-}Se)(\mu\text{-}PPh_2)$[μ-5-(2-pyridyl)-2-thienyl](CO)$_6$[P{5-(2-pyridyl)-2-thienyl}] were isolated as the major products. X-ray structural analysis of the former 50-electron cluster exhibits a bicapped, open triangular *nido* core, while the latter cluster is shown to consist of a Ru_3Se tetrahedron [65]. The reactivity of the 48-electron clusters $Ru_3(CO)_8(\mu\text{-}H)_2(\mu\text{-}PR_2)_2$ (where R = ^{t}Bu, Cy) towards phosphine ligands has been investigated. The Cy derivative was found to be much less reactive than the ^{t}Bu analogue. Whereas dppm and dppe react with $Ru_3(CO)_8(\mu\text{-}H)_2(\mu\text{-}P^tBu_2)_2$ to afford the 46-electron clusters $Ru_3(\mu\text{-}CO)(CO)_4(\mu_3\text{-}H)(\mu\text{-}H)(\mu\text{-}P^tBu_2)_2(\mu\text{-}P\text{–}P)$, the use of the phosphine ligands dmpm, dmpe, and P^nBu_3 furnish a complex mixture of products that could not be characterized. The X-ray structure of $Ru_3(CO)_6(\mu\text{-}H)_2(\mu\text{-}PCy_2)_2(Cy_2PH)_2$ has been determined, and the solution spectroscopic data for all new clusters are discussed [66]. The reaction between $dppfSe_2$ and $Ru_3(CO)_{12}$ has been reexamined. Thermolysis as a function of temperature affords the isomeric *nido* clusters $Ru_3(\mu_3\text{-}Se)_2(dppf)(CO)_7$ and $Ru_3(\mu_3\text{-}Se)_2(CO)_7(\mu\text{-}dppf)$, where the dppf ligand functions as a chelating and bridging ligand, respectively. The chelated species is obtained under kinetic control and is shown to convert to the bridging isomer under thermolysis in toluene. Also isolated from the thermolysis reactions is the cluster $Ru_3Se[\mu\text{-}P(Ph)C_5H_4Fe\text{-}C_5H_4PPh_2][\mu\text{-}C(O)Ph](CO)_6$, whose molecular structure exhibits a phosphido moiety and a benzoyl group. The redox behavior of these clusters has been studied by cyclic voltammetry [67]. Treatment of the nitrite cluster $Os_3(\mu\text{-}H)(CO)_{10}(\mu\text{-}\eta^2\text{-}NO_2)$ with dppf and *N*,*N*-dimethyl-1-[(*S*)-2-(diphenylphosphino)ferrocenyl]ethylamine in the presence of Me_3NO gives the bridged clusters $Os_3(\mu\text{-}H)(CO)_8(\mu\text{-}\eta^2\text{-}NO_2)(\mu\text{-}P\text{–}P)$ in moderate yields. X-ray analysis of both products confirms that the same Os–Os vector is spanned by the bridging hydride, diphosphine, and nitrite ligands. The redox properties of these clusters support a ferrocene-based HOMO and a LUMO that consists of contributions from the Os_3 core and the ferrocene ligand [68]. The synthesis and molecular structure of $H_2Ru_3(CO)_8(PCy_2)_2$ and $H_2Ru_3(CO)_6(PCy_2)_2(HPCy_2)_2$, which have been obtained from the reaction between $[HRu_3(CO)_{11}]^-$ and $HPCy_2$, are described. The former product exhibits a closed triangular Ru_3 core while the latter product reveals an open, almost linear Ru_3 skeleton. This same open-chain cluster is electron-deficient relative to conventional electron counting rules [69]. The bulky diphosphine ligands dcpm and F-dppe react with $Ru_3(CO)_{12}$ to afford $Ru_3(CO)_{12-x}(dcpm)_n$ and $Ru_3(CO)_{12-x}$(F-dppe)$_n$ (where $x = 2, 4$; $n = 1, 2$). The X-ray structures of $Ru_3(CO)_{12-x}(dcpm)_n$ and $Ru_3(CO)_{10}$(F-dppe) all show the expected $\mu_2\text{-}\eta^2$ coordination of the ancillary diphosphine ligand(s), with the cluster $Ru_3(CO)_8$(F-dppe)$_2$ showing both $\mu_2\text{-}\eta^2$ and $\mu_1\text{-}\eta^2$ diphosphine groups. The hydroformylation of ethylene and propylene using these clusters has been studied, and the observed catalytic activities were found to be higher than those observed by using $Ru_3(CO)_{12}$ and $Ru_3(CO)_{10}$(dppe) [70]. A report on the formation of heterocyclic phosphine ligands from the cluster-bound allenylidene complex $Ru_3(\mu\text{-}H)[\mu_3\text{-}C_2CH_2(OH)](CO)_9$ has appeared. Both dppm and dppe react with this cluster in the presence of $HBF_4 \cdot OMe_2$ to give clusters containing a diphosphacycloalkyne ligand as the result of double P-ligand attack on the C(1) and C(3) atoms of the allenylidene ligand. Both products were fully characterized in solution by IR and ^{31}P-NMR spectroscopies and their molecular structures were established by X-ray crystallography [71].

The thermolysis of $Os_3(CO)_{11}(AsPh_3)$ in refluxing nonane gives the following clusters as the major products $Os_3(\mu_3\text{-}AsPh)(\mu_3\text{-}\eta^2\text{-}C_6H_4)(CO)_9$, $Os_3(\mu\text{-}H)(\mu\text{-}AsPh_2)(\mu_3\text{-}\eta^2\text{-}C_6H_4)(CO)_9$, $Os_3(\mu\text{-}AsPh_2)_2(\mu_3\text{-}\eta^2\text{-}C_6H_4)\text{-}(CO)_7$, and $Os_3(\mu_3\text{-}AsPh)(\mu_3\text{-}\eta^2\text{-}C_6H_4)(CO)_8(AsPh_3)$. Each new cluster has been characterized in solution and by X-ray crystallography [72]. Thermolysis of the cluster $Os_3(CO)_{11}(SbPh_3)$ in octane yields the clusters $Os_3(\mu\text{-}SbPh_2)(\mu\text{-}H)(\mu_3\text{-}\eta^2\text{-}C_6H_4)(CO)_9$ and $Os_6(\mu_3\text{-}SbPh)(\mu_3\text{-}\eta^2\text{-}C_6H_4)(CO)_{20}$ as the initial products. Prolonged heating furnishes $Os_6(\mu_4\text{-}Sb)(\mu\text{-}H)(\mu_3\text{-}\eta^4\text{-}C_{12}H_8)(\mu_3\text{-}\eta^2\text{-}C_6H_4)(CO)_{16}$ as the major product. Heating the same starting cluster in a Carius tube at 115 °C gives the first two clusters along with $Os_6(\mu_4\text{-}Sb)(\mu\text{-}SbPh_2)(\mu\text{-}H)_2(\mu_3\text{-}\eta^4\text{-}C_{12}H_8)(\mu_3\text{-}\eta^2\text{-}C_6H_4)(CO)_{15}$, $Os_6(\mu_4\text{-}Sb)(\mu\text{-}SbPh_2)(\mu\text{-}H)(\mu_3\text{-}\eta^2\text{-}C_6H_4)_2(C_6H_5)(CO)_{16}$, and $Os_6(\mu_4\text{-}Sb)(\mu\text{-}SbPh_2)(\mu\text{-}H)(\mu_3\text{-}\eta^6\text{-}C_6H_4)(\mu_3\text{-}\eta^2\text{-}C_6H_4)\text{-}(C_6H_5)(CO)_{15}$. The relationship between these clusters is demonstrated, and the molecular structures of all of these products were established by X-ray crystallography [73]. The reactivity of 47-electron trihydrido(alkylidyne)triruthenium clusters has been explored. Chemical and electrochemical oxidation of the 48-electron clusters $H_3Ru_3(\mu_3\text{-}CX)(CO)_{9-n}L_n$ (where X = OMe, SEt, NMebz; L = various phosphines, $SbPh_3$) furnishes the corresponding radical cations,

which decompose via a disproportionation sequence involving the 48-electron precursor and an unknown 46-electron cluster species. The nature of the HOMO and LUMO levels in these clusters was also verified by Fenske-Hall MO calculations [74]. The unsaturated cluster $Os_3(CO)_8[Ph_2PCH_2P(Ph)C_6H_4](\mu\text{-}H)$ has been examined for its reactivity with a variety of thiols. Four X-ray structures accompany this report [75]. The formation and transformations of the σ-acetylide cluster $[Os_3(\mu\text{-}H)(CO)_{10}(PPh_3)(\sigma\text{-}C{\equiv}CCMe_2PPh_3)]^+$ and the isomeric clusters $[Os_3(\mu\text{-}H)(CO)_9(PPh_3)(\mu\text{-}\sigma{:}\eta^2\text{-}C{\equiv}CCMe_2PPh_3)]^+$ have been investigated. These clusters have been isolated from the reaction of $[Os_3(\mu\text{-}H)(CO)_{10}(\mu\text{-}\eta^1{:}\eta^2\text{-}{=}C{=}C{=}CMe_2]^+$ with PPh_3. These phosphonium complexes have been characterized fully by IR and NMR spectroscopies and by X-ray methods. Reaction pathways and reactivity schemes are discussed [76]. The dithiols $HS(CH_2)_nSH$ (where $n = 2$, 3) react with $(\mu\text{-}H)Os_3(CO)_8[Ph_2PCH_2P(Ph)C_6H_4]$ to produce $(\mu\text{-}H)Os_3(CO)_8[\mu\text{-}S(CH_2)_nS][Ph_2PCH_2P(Ph)C_6H_4]$ and $Os_3(CO)_8[\mu\text{-}S(CH_2)_nS](\mu\text{-}dppm)$. The former clusters contain 52-electrons and exhibit a bridging dithiolate and an orthometallated dppm ligand, and upon thermolysis, convert to the latter dppm-substituted clusters. Continued thermolysis of $Os_3(CO)_8[\mu\text{-}S(CH_2)_nS](\mu\text{-}dppm)$ leads to aliphatic C–H bond activation of the thiolato moiety and formation of $(\mu\text{-}H)Os_3(CO)_7(\mu_3\text{-}\eta^3\text{-}SCH_2CHS)(dppm)$ and $(\mu\text{-}H)Os_3(CO)_7(\mu_3\text{-}\eta^3\text{-}SCH_2CH_2CHS)(dppm)$. The X-ray structures of two products have been determined and their molecular structures are discussed relative to other structurally similar clusters [77]. Bidentate ligand isomerization via chelating and bridging intermediates has been demonstrated in the reaction of $Os_3(CO)_{10}(MeCN)_2$ with $Ph_2PCH_2CH_2SMe$. The cluster $1,2\text{-}Os_3(CO)_{10}(\mu\text{-}Ph_2PCH_2CH_2SMe)$ isomerizes slowly at room temperature to the chelating species $1,1\text{-}Os_3(CO)_{10}(Ph_2PCH_2CH_2SMe)$. Computational modeling reveals that both isomers possess similar stability, with the chelating isomer being slightly more stable. The kinetics associated with the isomerization have been measured by VT NMR spectroscopy, and the reaction was found to proceed via an associative process involving sulfur attack on an osmium center. The X-ray structures of $Os_3(CO)_{11}(Ph_2PCH_2CH_2SMe)$ and 1,2- and 1,1-$Os_3(CO)_{10}(Ph_2PCH_2CH_2SMe)$ (Fig. 6) have been solved, and the exchange pathways available to the ancillary CO groups have been investigated by ^{13}C-VT NMR spectroscopy [78].

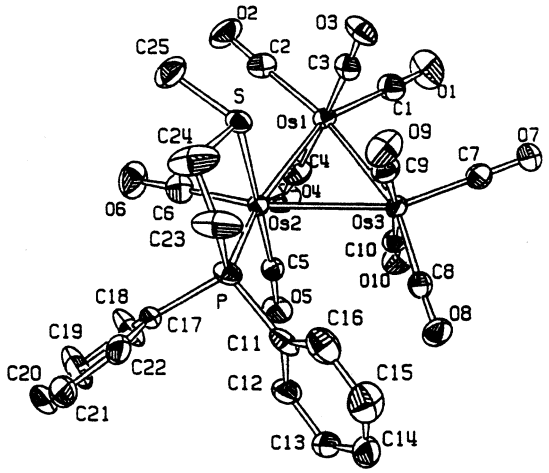

Fig. 6. X-Ray structure of $1,1\text{-}Os_3(CO)_{10}(Ph_2PCH_2CH_2SMe)$. Reprinted with permission from Organometallics. Copyright 2001 American Chemical Society.

The influence of Co and Ir on the ammonia synthesis over $[K]_2[Ru_4(CO)_{13}]$ has been studied. Both additives substantially decrease the ammonia synthesis rate [79]. $Cp^*_4Ru_4X_4$ (where X = Cl, Br) have been employed in the synthesis of novel diruthenium amidinate complexes [80]. Nucleophilic addition to the electron-deficient, 58-electron cluster $[H_4Ru_4(C_6H_6)_4]^{2+}$ has been explored. CO adds readily to the starting cluster to give the 60-electron cluster $[H_3Ru_4(C_6H_6)_4(CO)]^+$, while H_2O addition, which requires the presence of NaN_3 as a catalyst, and alcohol addition furnish the clusters $[H_3Ru_4(C_6H_6)_4(OH)]^+$ and $[H_3Ru_4(C_6H_6)_4(OR)]^+$, respectively. Two X-ray structures confirm the presence of a tetrahedral Ru_4 core and η^6-benzene ligands [81]. A report describing the electrospray ionization mass spectrum of $[Ru_4(\eta^6\text{-}C_6H_6)_4(OH)_4]^{4+}$ reveals that the main species present in aqueous solution is based on an intact cubane Ru_4 and the dimer $[Ru_2(\eta^6\text{-}C_6H_6)_2(OH)_2]^{2+}$. The role of the cubane cluster as a precatalyst in the hydrogenation of benzene is discussed [82]. Treatment of $Os_4(CO)_{12}(\mu\text{-}H)_4$ with Me_3NO, followed by 1,4-bis(ferrocenyl)butadiyne, produces $Os_4(CO)_{11}[\mu\text{-}\eta^2\text{-}FcCC(H)C_2Fc](\mu\text{-}H)_3$. The insertion of the butadiyne ligand into one of the Os–H bonds was verified by IR and ^1H-NMR spectroscopies and X-ray diffraction analysis. A tetrahedral core is found for the Os_4 atoms. The redox chemistry of this cluster indicates that there is little or no electronic interaction between the ferrocenyl moieties [83]. The new osmium clusters $Os_4(\mu\text{-}H)_4(CO)_{11}[\eta^1\text{-}NC_5H_5(N{=}N)Ph]$ and $Os_4(\mu\text{-}H)_4(CO)_{10}[\eta^2\text{-}NC_5H_4(N{=}N)Ph]$ have been synthesized from $Os_4(\mu\text{-}H)_4(CO)_{12}$ and 2-phenylazopyridine. The former product transforms into the latter product upon thermolysis and CO loss. The coordination chemistry of the 3-phenylazopyridine with $Os_4(\mu\text{-}H)_4(CO)_{12}$ has also been studied. Four X-ray structures accompany this report [84]. Thermolysis of $Ru_2(\mu\text{-}\eta^1{:}\eta^1\text{-}N{=}CPh_2)(\mu\text{-}\eta^1{:}\eta^2\text{-}PhC{=}CHPh)(CO)_6$ is reported to give a tetranuclear species having the formula $Ru_4C_{48}H_{30}N_2O_8$, whose molecular structure could not be determined [85]. A study on the electron-donating capacity of the μ_4-P moiety in $Ru_4(CO)_{12}(\mu\text{-}PF_2)(\mu_4\text{-}P)$ has been published. The role of the phosphinidene moiety as a 3-electron or a 5-electron-donor has been addressed through X-ray

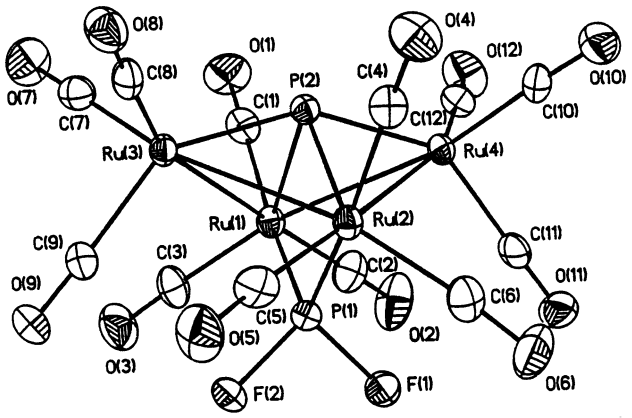

Fig. 7. X-Ray structure of $Ru_4(CO)_{12}(\mu\text{-}PF_2)(\mu_4\text{-}P)$. Reprinted with permission from Organometallics. Copyright 2001 American Chemical Society.

structural studies and DFT calculations. The X-ray structure of $Ru_4(CO)_{12}(\mu\text{-}PF_2)(\mu_4\text{-}P)$ exhibits an opened Ru_4 butterfly core with no Ru–Ru bonding in the hinge vector (Fig. 7). The MO data on $Ru_4(CO)_{12}(\mu\text{-}PF_2)(\mu_4\text{-}P)$ are contrasted with other structurally similar clusters of varying electron counts [86].

The unstable pentaruthenium boride cluster $[Ru_5(CO)_{15}B]^-$ has been prepared from $[Ru_6(CO)_{17}B]^-$. Cluster stabilization has been demonstrated by coordination to gold(phosphine) fragments to give $Ru_5(CO)_{15}BAuPR_3$ (where R = Ph, *o*-tolyl). Treatment of $[Ru_5(CO)_{15}B]^-$ with $[(Ph_3PAu)_3O][BF_4]$ furnishes $Ru_5(CO)_{14}B(AuPPh_3)_3$, whose molecular structure has been solved and is discussed relative to other Ru_5B clusters [87]. The clusters $Os_5(\mu\text{-}X)_2(CO)_{16}(CN^tBu)$ (where X = Cl, Br) have been synthesized from $Os_3(\mu\text{-}X)_2(CO)_{10}$ and $Os(CO)_4(CN^tBu)$. The X-ray structure of the chloro derivative reveals that the original $Os_3(\mu\text{-}Cl)_2$ fragment is maintained with a coordination site *cis* to the Cl ligands occupied by the $Os(CO)_4Os(CO)_3(CN^tBu)_2$ moiety. The 'hook' orientation exhibited by the Os_5 core is the first of its kind. The dative Os–Os bonds in the pendant moiety are discussed [88]. The reversible interconversion of a C_{60} ligand between $\mu,\eta^2{:}\eta^2$ and $\mu_3,\eta^2{:}\eta^2{:}\eta^2$ coordination modes on a pentaosmium cluster has been reported. Decarbonylation of $Os_5C(CO)_{14}(PPh_3)$ by Me_3NO (2 equiv.), followed by refluxing in chlorobenzene with C_{60}, gives $Os_5C(CO)_{11}(PPh_3)(\mu_3,\eta^2{:}\eta^2{:}\eta^2\text{-}C_{60})$. Treatment of this cluster with CO at 80 °C furnishes $Os_5C(CO)_{12}(PPh_3)(\mu,\eta^2{:}\eta^2\text{-}C_{60})$ in good yield. Further thermolysis at 132 °C under an inert atmosphere regenerates the original C_{60}-substituted cluster. The ligand substitution chemistry of these clusters with benzyl isocyanide and the reactivity of the Ru_5 carbide analogues are described. Five X-ray structures have been determined and are discussed [89].

The cluster $Ru_6C(CO)_{17}$ has been attached to Argo-Gel polymer beads via phosphine ligands and crown ether interactions with ammonium salt functionalities. The hydrogenation activity of the immobilized clusters was explored [90]. The preparation of $[Ru_6C(CO)_{16}SnCl_3]^-$ and $Ru_6C(CO)_{16}SnCl_2$ is described, along with the use of these clusters as supported catalysts on mesoporous silica. The supported-cluster structure retains its integrity, as evidenced by FTIR and EXAFS measurements, up to around 200 °C [91]. A study on laser desorption ionization versus electrospray ionization mass spectrometry has been published. Some of the cluster systems examined include $[HRu_6(CO)_{18}]^-$, $[Ru_6C(CO)_{16}]^{2-}$, $[Re_8C(CO)_{24}]^{2-}$, and $[Os_{10}C(CO)_{24}]^{2-}$. The different information afforded by each technique is discussed [92]. Ring expansion via metal–metal bond cleavage in $Os_6(\mu_4\text{-}Sb)(\mu\text{-}H)_2(\mu\text{-}SbPh_2)(\mu_3,\eta^2\text{-}C_6H_4)(\mu_3,\eta^4\text{-}C_{12}H_8)(CO)_{15}$ occurs upon treatment with CN^tBu. The clusters isolated, $Os_6(\mu_4\text{-}Sb)(\mu\text{-}H)(\mu\text{-}SbPh_2)(C_6H_5)(\mu_3,\eta^4\text{-}C_{12}H_8)(CO)_{14}(CN^tBu)_2$ and $Os_6(\mu_4\text{-}Sb)(\mu\text{-}H)(\mu\text{-}SbPh_2)(C_6H_5)(\mu_3,\eta^4\text{-}C_{12}H_8)(CO)_{15}(CN^tBu)_3$, have been fully characterized in solution and by X-ray crystallography. Both products contain five-membered Os_3Sb_2 rings [93]. New routes to the high-nuclearity clusters $[H_5Os_{10}(CO)_{24}]^-$ and $[H_4Os_{10}(CO)_{24}]^{2-}$ from the hydrogenation of silica-supported $[Os(CO)_3(OH)_2]_n$ are described. The decaosmium clusters are obtained at 200 °C using ethylene glycol as a solvent. $\alpha\text{-}[Os(CO)_3Cl_2]_2$ may also be employed as a starting material for the synthesis of these new Os_{10} clusters [94].

2.4. Group 9 clusters

The tricobalt cluster $Co_3(\mu_3\text{-}S)(\mu\text{-}CNEt_2)(\mu\text{-}SCNEt_2)_2(PPh_3)(Cl)$ has been isolated from the reaction of $CoCl_2$, PPh_3, and diethyldithiocarbamate in the presence of zinc powder. The single and double C–S bond cleavage in the product has been crystallographically established [95]. The synthesis of cyclopentadienones via the intramolecular [2+2+1]-cocyclization of diynes and CO has been achieved with the catalysts $RCCo_3(CO)_9$. The most active catalyst precursor was found to be the methylidynetricobalt cluster $HCCo_3(CO)_9$ [96]. Treatment of the bis(μ-thiolato)dicobalt complex $Co_2Cp_2(\mu\text{-}SMe)_2$ with $Co_2(CO)_6(\mu\text{-}F_3CC{\equiv}CH)$ yields the clusters $Co_3Cp(CO)_4(\mu\text{-}SMe)_2(\mu\text{-}F_3CC{\equiv}CH)$ (two isomers) and $Co_3Cp_2(CO)_3(\mu\text{-}SMe)(\mu\text{-}F_3CC{\equiv}CH)$. The X-ray structure of one of the cluster isomers reveals that it possesses a triangular array of cobalt atoms and 50-valence electrons. The latter 50-electron cluster contains an open-chain of cobalt atoms. The VT NMR behavior of these clusters has been explored, and the fluxional pathways between the different isomeric forms of these clusters are discussed [97]. The reaction between K_3AsS_2 and $CpCo(CO)I_2$ (where Cp = Cp*,

C_5Me_4Et) in DMF at 120 °C gives $Cp_2Co_2As_2S_3$, $[Cp_3Co_3AsS_6]^+$, and $[Cp_3Co_3AsS_5]^+$. The structures of two products are presented and discussed [98]. Methylidene and hydrazone compounds based on $Cp_3MCo_2(CO)_3$ are reported. The X-ray structures of $Cp_3Co_3(\mu\text{-}CO)_2(\mu_2\text{-}CH_2)$ and $Cp_3Co_3(\mu_3\text{-}CO)(\mu_3\text{-}NNCH_2)$ have been determined, and the dynamic behavior of the methylidene ligand in these derivatives has been studied by detailed NMR measurements [99]. Me_3NO activation of $PhCCo_3(CO)_9$ in the presence of the diphosphine ligand bpcd affords the thermally unstable cluster $PhCCo_3(CO)_7$(bpcd). Thermolysis of this bpcd-substituted cluster gives the phosphido-bridged species $Co_3(CO)_6[\mu_2\text{-}\eta^2\text{:}\eta^1\text{-}C(Ph)\text{-}C{=}C(PPh_2)C(O)CH_2C(O)](\mu_2\text{-}PPh_2)$ in a process involving a rate-limiting loss of CO. Three isomers of $PhCCo_3(CO)_7$(bpcd) were observed in solution at low-temperature by ^{31}P-NMR spectroscopy. The X-ray structures of both products were crystallographically established, and the molecular structures have been discussed relative to other Co_3 clusters of this genre [100].

Immobilized metallic nanoparticles capable of hydrogenating aromatic C–C bonds have been obtained from heating sol–gel entrapped $Rh_2Co_2(CO)_{12}$ [101]. The reactivity of site-isolated metal clusters in alkene hydrogenation has been studied. Treatment of porous γ-Al_2O_3 with $Ir_4(CO)_{12}$ affords the supported catalyst system, whose composition was determined by IR and ^{13}C-NMR methods, and EXAFS measurements [102]. The reaction between $Rh_4(CO)_{12}$ and cot and 1,4-$(Me_3Si)_2C_8H_6$ gives facially coordinated cyclooctatetraene ligands. Thermolysis in boiling pentane yields $Rh_4(CO)_8(\mu_3\text{-}C_8H_8)$, while reaction in refluxing heptane produces the bis-cot cluster $Rh_4(CO)_6(\mu_3\text{-}C_8H_8)(\eta^4\text{-}C_8H_8)$. The X-ray structures of five Rh_4 clusters have been solved and their molecular structures are discussed [103]. Discrete mixed-valence metal chains containing iridium pyridonate blues have been synthesized from $[Ir(\mu\text{-}OPy)(CO)_2]_2$. Oxidation of this dimer with molecular iodine gives a blue solid of HH,HT-$[\{Ir_2(\mu\text{-}OPy)_2(I)(CO)_4\}_2]$, which is shown to transform into the corresponding thermodynamically stable HH,HH isomer. X-ray structural analyses on both isomers verify the near-linear chain arrangement of the four iridium atoms [104]. The synthesis and structure of the tetrarhodium icosahedral metallacarborane cluster $[Rh(\eta^5\text{-}Ph_2C_2B_9H_9)(\mu_3\text{-}OH)]_4$ have been published [105]. The preparation and molecular structures of $Co_4(\mu\text{-}dppm)_2(\mu\text{-}CO)_3(CO)_5$ and $Co_4(\mu\text{-}CO)_3(CO)_6(\eta\text{-}C_6H_6)$ have been described. Each cluster contains a tetrahedral Co_4 core, where one face is edge-bridged by three μ-CO ligands [106]. Thermolysis of $Co_4(\mu_3\text{-}AsPh)(\mu_4\text{-}\eta^2\text{:}\eta^2\text{:}\eta^1\text{-}As_4Ph_4)(\mu\text{-}CO)_2(CO)_8$ in benzene affords $Co_4(\mu_3\text{-}AsPh)_2(\mu_4\text{-}\eta^2\text{:}\eta^1\text{-}As_2Ph_2)(\mu\text{-}CO)(CO)_9$. Fragmentation of the tetraarsine chain in the starting cluster is also observed when the cluster is refluxed with added $Fe_2(CO)_9$. The major cluster product isolated from this reaction has been identified as $Co_4(\mu_3\text{-}AsPh)_2[(\mu_4\text{-}\eta^2\text{:}\eta^1\text{-}As_2Ph_2)Fe(CO)_4](\mu\text{-}CO)(CO)_9$. CO substitution in the same starting cluster by $P(OMe)_3$ occurs in refluxing benzene to give $Co_4(\mu_3\text{-}AsPh)(\mu_4\text{-}\eta^2\text{:}\eta^2\text{:}\eta^1\text{-}As_4Ph_4)(\mu\text{-}CO)_2(CO)_5[P(OMe)_3]_3$. Each product cluster was subjected to X-ray structural analysis [107]. Condensation of $[HIr_4(CO)_{11}]^-$ with $[Ir(CO)_4]^-$ furnishes $[HIr_5(CO)_{12}]^{2-}$ in nearly quantitative yield. X-ray diffraction analysis reveals the existence of a trigonal-bipyramidal arrangement of iridium atoms. PPh_3 reacts with $[HIr_4(CO)_{11}]^-$ to give $[HIr_4(CO)_{10}(PPh_3)]^-$ without any trace of polysubstitution. The solution isomers of this cluster have been examined by ^{1}H- and ^{31}P-NMR spectroscopies [108].

Pentametallic cobalt clusters that have the general formula $Co_5(CO)_{12}(C{\equiv}CR)$ have been synthesized from $Co_2(CO)_8$ and $BrC{\equiv}CR$. Solution IR and NMR data for these clusters are presented [109].

The ligand effects on the structures of $Rh_6(CO)_{15}L$ (where L = various donor ligands) have been explored by X-ray crystallography. All of the monosubstituted clusters exhibit structures based on an octahedral array of rhodium atoms and are remarkably similar to the parent cluster $Rh_6(CO)_{16}$, whose X-ray structure was also redetermined [110]. The stereochemical nonrigidity of $Rh_6(CO)_{15}L$ has been studied by VT and 2-D (^{13}C-, ^{103}Rh-, ^{31}P–^{103}Rh; HMQC; ^{13}C-EXSY) NMR methods. At low-temperatures the spectra are consistent with the solid-state structure of each cluster. The localized exchanges of terminal and face-bridging CO groups are discussed as a function of temperature [111]. 1- and 2-D-NMR data on the ligand fluxionality in $[Rh_6C(CO)_{14}(PPh_3)]^{2-}$ have been reported. Intermolecular exchange with ^{13}CO is shown to be related to the value of ^1J(Rh–CO), with the edge-bridging CO's undergoing a faster reaction than the terminal CO groups [112]. The reaction between $[Co(CO)_4]^-$ and PCl_5 in refluxing THF produces $[Co_9P(CO)_{21}]^{2-}$, whose X-ray structure (Fig. 8) consists of a monocapped square antiprismatic cobalt core with an interstitial phosphide moiety. Reaction with CO affords $[Co_9P(CO)_{22}]^{2-}$, which is not stable and decomposes to the starting cluster and $[Co(CO)_4]^-$. The structure of $[Co_9P(CO)_{22}]^{2-}$ is based on a bicapped antiprismatic array of cobalt atoms and a cobalt-encapsulated phosphide group [113].

2.5. Group 10 clusters

The unstable clusters $Pt_3(CO)_3(PR_3)_3(\mu_3\text{-alkyne})$ have been synthesized from $Pt_3(\mu\text{-}CO)_3(PR_3)_3$ and alkynes. In the case of the ^{t}BuO$_2$CC≡CCO$_2^t$Bu derivative, the stereochemistry of the unstable cluster has been deter-

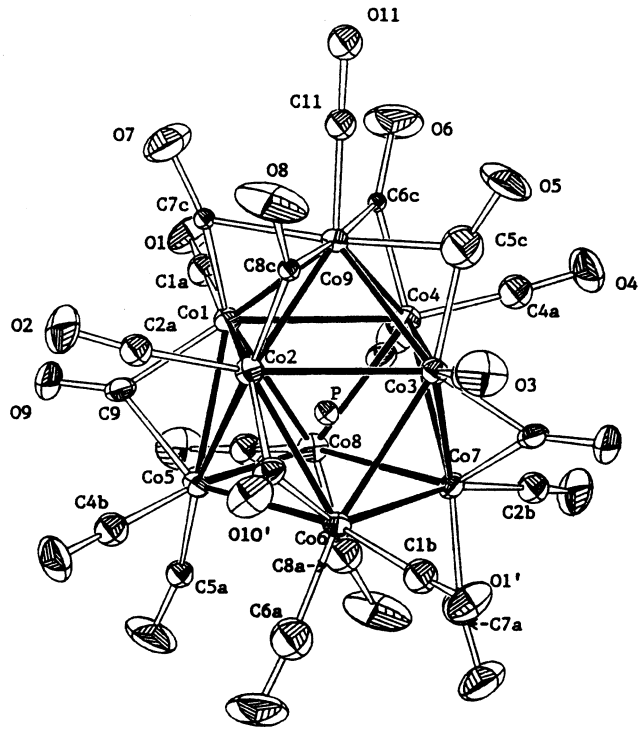

Fig. 8. X-Ray structure of $[Co_9P(CO)_{21}]^{2-}$. Reprinted with permission from Inorganic Chemistry. Copyright 2001 American Chemical Society.

mined by low-temperature NMR measurements [$^{195}Pt\{^1H\}$, $^{31}P\{^1H\}$, $^{13}C\{^1H\}$]. At elevated temperatures, alkyne scrambling about the cluster core renders all three platinum atoms equivalent on the NMR time scale. Decomposition of the triplatinum clusters takes place at room temperature and affords the stable dinuclear complexes $Pt_2(CO)_2(PR_3)_2(\mu\text{-alkyne})$ [114]. Kinetic studies on the redox reactions of $[Pt_3(CO)_6]_n^{2-}$ (where $n = 3$, 4, 5) with H_2 and acid have been carried out, and the data are discussed with respect to the aggregate state of the cluster [115]. The reactivity of alkenes with $Pt_3(\mu\text{-}CO)_3(PR_3)_3$ has been investigated. Quantitative formation of $Pt_3(\mu\text{-}CO)_3(PR_3)_3(\text{alkene})$ is observed at low-temperature, with decomposition to $Pt(CO)(PR_3)(\text{alkene})$ being found at room temperature. NMR and IR spectroscopic data on the intermediates and end products are presented and discussed [116]. A report on the electrochemically induced C–Br and C–I bond cleavage in RX compounds by $[Pd_3(dppm)_3(CO)]^{2+}$ has appeared. The intermediate cluster $[Pd_3(dppm)_3(CO)(CF_3CO_2)]^+$, which represents the first spectroscopically characterized paramagnetic palladium cluster, is able to react with alkyl halides to give $[Pd_3(dppm)_3(CO)(X)]^+$ and 'R^+'. These reactions have been studied by cyclic voltammetry, coulometric methods, and EPR spectroscopy [117]. The mechanism associated with the protonation of $Pt_3(\mu\text{-}P^tBu_2)_3(H)(CO)_2$ has been examined. The hydride-bridged complex $[Pt_3(\mu\text{-}P^tBu_2)_2(\mu\text{-}H)(P^tBu_2H)(CO)_2]^+$ has been verified by spectroscopic methods. Use of TfOD as the acid gives selectively $[Pt_3(\mu\text{-}P^tBu_2)_2(\mu\text{-}D)(P^tBu_2H)(CO)_2]^+$, which indicates that the proton is transferred to a platinum center while the P–H bond is formed via reductive coupling of one of the bridging phosphido groups and the terminal hydrogen. The results of an ab initio MO study are presented and discussed [118]. Synthetic methods leading to heterotrinuclear palladium(II)/platinum(II) clusters with bridging phosphido groups are described. The compounds have the general formula $[(C_6F_5)_2M(\mu\text{-}PPh_2)_2M'(\mu\text{-}PPh_2)_2M''(C_6F_5)_2]^{2-}$ [where M, M′, M″ = Pd(II), Pt(II)]. The redox chemistry of these clusters has been explored, and the data from MO calculations at the B3LYP level are presented [119]. The formation of $[(C_6F_5)(PPh_3)Pt(\mu\text{-}PPh_2)(\mu\text{-}H)]_2Pt$ from the reaction between *cis*-$Pt(C_6F_5)_2(PPh_2H)_2$, $Pt(\text{norbornene})_3$, and PPh_3 has been reported. The X-ray structure and spectroscopic data of this triplatinum chain cluster are discussed [120]. Unsymmetrical A-frame Pt_2Pd trinuclear complexes, formed by site-selective, double insertion of alkynes into Pd–Pt and Pd–P bonds, have been prepared and characterized by X-ray crystallography. Four X-ray structures accompany this report, of which $[Pt_2Pd(\mu\text{-dpmp})\{\mu\text{-}PPh_2CH_2P(Ph)CH_2P(Ph)_2CHC(CO_2Me)\}(XylNC)_2]^{2+}$ is shown in Fig. 9 [121].

Cluster expansion reactions have furnished $[Pt_4(\mu\text{-}CO)_3(\mu\text{-dppm})_3(PPh_3)]^{2+}$ and $[Pt_4(\mu\text{-H})(\mu\text{-}CO)_2(\mu\text{-dppm})_3(PPh_3)]^+$ from $[Pt_3(\mu_3\text{-}CO)(\mu\text{-dppm})_3]^{2+}$ and $[Pt_3(\mu_3\text{-H})(\mu\text{-dppm})_3]^+$, respectively, upon treatment with the platinum fragment $Pt(CO)_2(PPh_3)$. Both Pt_4 clusters contain 58-electrons, possess butterfly structures, and are fluxional in solution [122]. The synthesis and characterization of the first platinum formyl complex have been described. Treatment of $[Pt_6(CO)_6(\mu\text{-}P^tBu_2)_4]^{2+}$, which was prepared from $Pt_3(H)(CO)_2(\mu\text{-}$

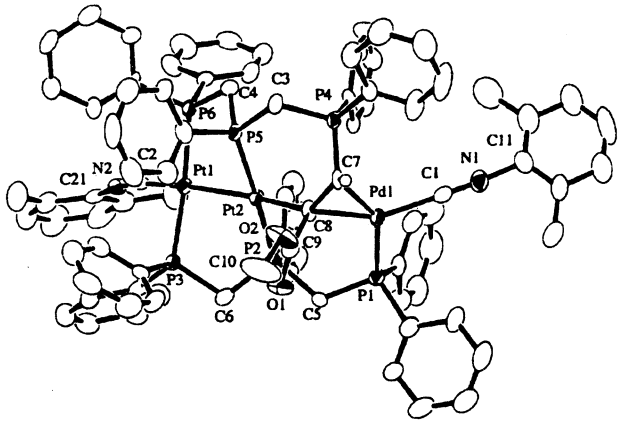

Fig. 9. X-Ray structure of $[Pt_2Pd(\mu\text{-dpmp})\{\mu\text{-}PPh_2CH_2P(Ph)CH_2P(Ph)_2CHC(CO_2Me)\}(XylNC)_2]^{2+}$. Reprinted with permission from Organometallics. Copyright 2001 American Chemical Society.

$P^tBu_2)_3$ and excess triflic acid under CO, with $NaBH_4$ yields the bis(formyl) cluster $Pt_6(CO)_4(CHO)_2(\mu\text{-}P^tBu_2)_4$. While thermally robust at room temperature, the cluster undergoes decarbonylation at 60 °C to give the corresponding dihydrido cluster $Pt_6(CO)_4(H)_2(\mu\text{-}P^tBu_2)_4$. The molecular structure of the parent Pt_6 cluster has been determined by X-ray crystallography [123]. The tetraplatinum bis(μ-alkynyl)bis(μ-dppa) clusters $[(C_6F_5)_2Pt(C{\equiv}CR)_2Pt(\mu\text{-dppa})]_2$ have been synthesized and fully characterized in solution [124].

The cluster compounds $[Ni_{36}Pt_4(CO)_{45}]^{6-}$ and $[Ni_{37}Pt_4(CO)_{46}]^{6-}$ have been obtained from the reaction of $[Ni_6(CO)_{12}]^{2-}$ with K_2PtCl_4. The metal core of the $Ni_{36}Pt_4$ cluster exhibits a Pt_4 tetrahedron fully encapsulated in a shell of 36 Ni atoms that belong to a distorted and incomplete v_5 tetrahedron. The $Ni_{37}Pt_4$ cluster reveals a similar molecular polyhedron with the unique triangular face of the metal polyhedron being capped by the additional Ni(CO) fragment. Both clusters undergo rapid degradation under CO to produce the known cluster $[Ni_9Pt_3(CO)_{21}]^{4-}$. The electrochemical properties of these clusters have also been investigated [125]. The four high-nuclearity clusters $Pd_{16}(CO)_{13}(PMe_3)_9$, $Pd_{35}(CO)_{23}(PMe_3)_{15}$, $Pd_{39}(CO)_{23}(PMe_3)_{16}$, $Pd_{59}(CO)_{32}(PMe_3)_{21}$, and $Pd_{29}Ni_3(CO)_{22}(PMe_3)_{13}$ have been synthesized and structurally characterized. The different icosahedral-based frameworks exhibited by these clusters are discussed, and proposed growth sequences for the logical assembly of these clusters via the centered Pd_{13} icosahedral fragment in $Pd_{16}(CO)_{13}(PMe_3)_9$ are presented [126]. The synthesis and X-ray structures of $[Ni_{24}Pt_{14}(CO)_{44}]^{4-}$ and $[Ni_{10}(Ni_{6-x}Pt_x)Pt_8(CO)_{30}]^{4-}$ (where $x \approx 2$) have been published. The latter cluster reveals a localized substitutional Ni/Pt disorder and an unprecedented close-packed metal framework. Extended Hückel calculations have been carried out and well-defined HOMO–LUMO levels in each cluster were not observed [127]. The heteropalladium clusters $[Pd_{16}Ni_4(CO)_{22}(PPh_3)_4]^{2-}$ and $[Pd_{33}Ni_9(CO)_{41}(PPh_3)_6]^{4-}$ have been isolated as the major products from the reaction between $PdCl_2(PPh_3)_2$ and $[Ni_6(CO)_{12}]^{2-}$. Pseudo-T_d ccp $Pd_{16}Ni_4$ and pseudo-D_{3h} hcp $Pd_{33}Ni_9$ cores have been crystallographically established via CCD X-ray analyses. Spectroscopic data and VT magnetic susceptibility data are presented and discussed [128].

2.6. Group 11 clusters

The synthesis and luminescent properties of $[Cu_3(\mu\text{-dppm})_3(\mu_3\text{-}\eta^1\text{-}C{\equiv}C\text{-benzo-15-crown-5})_2]^+$ are reported. Sodium ion-binding of the crown ether has been studied by electrospray ionization-mass spectrometry and emission spectroscopy. X-ray structural analysis of this cluster reveals the presence of a near planar Cu_3P_6 core [129]. The reaction between $[Au(C_6F_5)_2\{2\text{-(diphenylphosphino)aniline}\}]^+$ and $Au(acac)(PPh_3)$ yields the trinuclear complex $[Au(C_6F_5)_2\{2\text{-(diphenylphosphino)aniline}(AuPPh_3)_2\}]^+$, whose X-ray structure is based on a Au_3 core. The unusual Au(I)–Au(III) interaction present in product is discussed with respect to related mixed-valence gold complexes [130]. Mixed gold(I)–gold(III) complexes possessing bridging selenido ligands have been prepared and structurally characterized. The reaction of $Se(AuPPh_3)_2$ and $Se[Au_2(\mu\text{-dppf})]$ with $Au(C_6F_5)_3(OEt_2)$ affords $Se(AuPPh_3)_2[Au(C_6F_5)_3]_n$ and $[Se\{Au_2(\mu\text{-dppf})\}\{Au(C_6F_5)_3\}_n]$ (where $n = 1$, 2). The related compound $[\{Se(AuPPh_3)\}_2\{\mu\text{-}Au(C_6F_5)_2\}_2]$ has been obtained from the reaction between $Se(AuPPh_3)_2$ and $[Au(C_6F_5)_2Cl]_2$. The Au(I)–Au(III) interactions in these systems have been analyzed via quasi-relativistic pseudopotential calculations [131]. The synthesis and X-ray structure of the rhombohedral silver-alkynyl cage compound $[Ag_{14}(C{\equiv}C^tBu)_{12}Cl]^+$ have been published [132].

3. Heterometallic clusters

3.1. Trinuclear clusters

The bimetallic complex $Cp_2Ti(\mu_2\text{-}SH)_2RuClCp^*$ has been allowed to react with $RuCl_2(PPh_3)_3$ and $M_2(cod)(\mu_2\text{-}Cl)_2$ (where M = Rh, Ir) in the presence of Et_3N to produce $(CpTi)(Cp^*Ru)[Ru(PPh_3)_2](\mu_3\text{-}S)_2(\mu_2\text{-}Cl)_2$ and $(CpTi)(Cp^*Ru)[M(cod)](\mu_3\text{-}S)_2(\mu_2\text{-}Cl)_2$, respectively. The same TiRu starting compound reacts with $M'(PPh_3)_4$ (where M′ = Pd, Pt) to give the TiRuM′ clusters $(CpTi)(Cp^*Ru)[M'(PPh_3)_2](\mu_3\text{-}S)(\mu_2\text{-}S)(\mu_2\text{-}H)$, which contain an unprecedented $M_3(\mu_3\text{-}S)(\mu_2\text{-}S)$ core. Three X-ray structures have been determined, and the structural features are discussed [133].

The reactivity of the isomeric clusters $[Cp^*Ru(CO)_2]_2[W(\mu\text{-}S)_4]$ and $[Cp^*Ru(CO)_2]_2[W(=S)(\mu_3\text{-}S)(\mu\text{-}S)_2]$ with $PtMe_2(cod)$ has been investigated. The major products were found to be $[Cp^*Ru(CO)_2]_2[W(\mu_3\text{-}S)_2(\mu\text{-}S)_2](PtMe_2)$ and $[Cp^*Ru(CO)_2]_2[W(=S)(\mu_3\text{-}S)_3](PtMe_2)$. Use of two equivalents of $PtMe_2(cod)$ with $[Cp^*Ru(CO)_2]_2[W(\mu\text{-}S)_4]$ furnishes the pentametallic cluster $[Cp^*Ru(CO)_2]_2[W(\mu_3\text{-}S)_4](PtMe_2)_2$. The monochlorination of the these products upon treatment with HCl has also been examined. The X-ray structures of three clusters are presented and discussed [134]. Selective CO substitution by cyclohexyl isocyanide in $(\eta^5\text{-}C_5H_4R)FeMCo(CO)_8(\mu_3\text{-}S)$ (where M = Mo, W; R = MeCO, MeO_2C) has been demonstrated. The mono-substituted clusters reveal that the incoming ligand is attached to the Group 6 metal, while the disubstituted clusters possess iron-bound and Group 6-bound isocyanide ligands. Prolong stirring of the starting clusters with excess isocyanide affords the tris-substituted clusters $(\eta^5\text{-}C_5H_4R)FeMCo(CO)_5(CyNC)_3$-

(μ_3-S), in which each metal atom is substituted by an isocyanide ligand. The molecular structures of four products have been solved by X-ray analysis [135]. The use of bis(*p*-methoxyphenyl)telluroxide as an oxygen-transfer reagent and donor ligand in the reaction with (μ_3-S)$FeCo_2(CO)_9$ is described. The clusters (μ_3-S)$FeCo_2(CO)_{9-n}[(p\text{-}MeOC_6H_4)_2Te]_n$ (where $n = 1$, 2) have been isolated and studied for their reactivity with added PPh_3. The cluster compounds (μ_3-E)$FeCoM(CO)_8(\eta^5\text{-}C_5H_4R)$ (where E = S, Se; R = H, MeCO, MeO_2C; M = Mo, W) have been examined for their reactivity towards the tellurium-oxide reagent. The X-ray structures of (μ_3-S)$FeCoMo(CO)_7[\eta^5\text{-}C_5H_4C(O)Me](PPh_3)$ and (μ_3-Se)$FeCoMo(CO)_7[\eta^5\text{-}C_5H_4C(O)Me](PPh_3)$ have been solved and their important features fully discussed [136]. The synthesis and redox properties of tetrahedral clusters containing $Mo_2Fe(\mu_3\text{-}S)$ cores and macrocyclic crown ether ligands have been studied. Included in this report are the X-ray structures of $[Mo_2Fe(\mu_3\text{-}S)(CO)_7][\eta^5\text{-}C_5H_4CH_2(CH_2OCH_2)_nCH_2C_5H_4\text{-}\eta^5]$ (where $n = 1$–3) [137]. The synthesis and reactions of (μ_3-S)FeCoMo and (μ_3-Se)FeCoMo tetrahedral clusters containing $(p\text{-}MeC_6H_4)_2Te$ ligands are described [138]. Treatment of $FeCo_2(CO)_9(\mu_3\text{-}S)$ with $[M(CO)_3\{\eta^5\text{-}C_5H_4C(O)CH_2CH_2CO_2Me\}]^-$ (where M = Mo, W) leads to the formation of the chiral clusters (μ_3-S)$CoFeM(CO)_8[\eta^5\text{-}C_5H_4C(O)CH_2CH_2CO_2Me]$, which undergo reactions with various amines to produce hydrazone derivatives [139]. The dinuclear complex $Cp_2(OC)_4Mo_2(\mu\text{-}PH_2)(\mu\text{-}H)$ reacts with $Mn_2(CO)_{10}$ to give the trinuclear complex $[Cp(OC)_2Mo]_2PMn(CO)_4$, whose molecular structure (Fig. 10) reveals the presence of a triply metallated sp-phosphorus atom that is tethered by all three metals. $Re_2(CO)_{10}$ reacts with the Mo_2 dimer in an analogous fashion. Treatment of $Cp_2(OC)_4Mo_2(\mu\text{-}PH_2)(\mu\text{-}H)$ with $M_3(CO)_{12}$ (where M = Fe, Ru) gives the tetrametallic clusters $Cp(OC)_8M_2[\mu_3\text{-}PMoCp(CO)_3](\mu\text{-}H)$ and $Cp_2(OC)_7Mo_2M[\mu_3\text{-}PMoCp(CO)_3]$. The spectroscopic data and diffraction data for three new clusters are discussed [140].

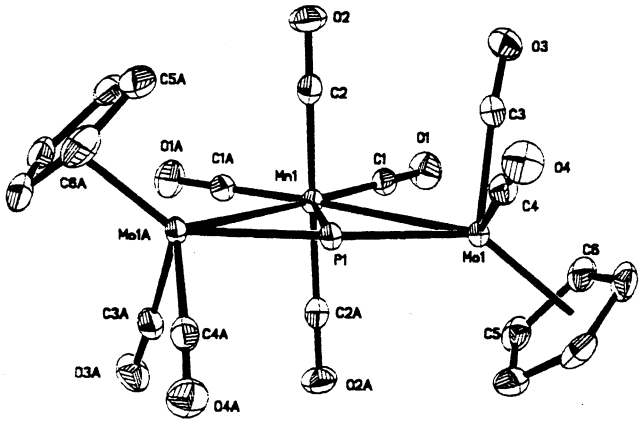

Fig. 10. X-Ray structure of $[Cp(OC)_2Mo]_2PMn(CO)_4$. Reprinted with permission from Organometallics. Copyright 2001 American Chemical Society.

The reaction between $Fe_3(CO)_9(\mu_3\text{-}X)_2$ (where X = S, Se) and $CpCr(CO)_2(\eta^3\text{-}P_3)$ in the presence of Me_3NO gives the clusters $Fe_2(CO)_6(\mu_3\text{-}X_3P)[CpCr(CO)_2]$, whose molecular structures consist of a butterfly-like $Fe_2(CO)_6X_2$ unit and a $CpCr(CO)_2X$ moiety connected by a μ_4-P bridging ligand that is bonded to all three chalcogenides atoms and the chromium center [141]. The μ_3-alkylidyne-capped cluster $NiMo_2(\mu_3\text{-}CCH_2CO_2Me)(CO)_4Cp^*Cp_2$ has been isolated and structurally characterized from the reaction of methyl acrylate and the heterobimetallic complex Cp*Ni=Mo(μ-CO)$(CO)_2Cp$. The $NiMo_2$ cluster results from a double C–H bond activation of the CH_2 group of the methyl acrylate. When the homodinuclear complexes $[Cp^*Ni(\mu\text{-}CO)]_2$, $[CpMo(CO)_3]_2$, and $Cp(OC)_2Mo{\equiv}Mo(CO)_2Cp$ were allowed to react with methyl acrylate, no trinuclear clusters were found [142]. The new 44-electron clusters $Pt_2M(\mu\text{-}CO)_3(\mu\text{-}PPh_2)Cp(PPh_3)$ (where M = Mo, W) and $Pt_3(\mu\text{-}CO)_2(\mu\text{-}PPh_2)(I)(PPh_3)$ have been synthesized from $Pt_2(\mu\text{-}H)(\mu\text{-}PPh_2)I_2(PPh_3)_2$ and the carbonylmetallates $[CpM(CO)_3]^-$ and $[Co(CO)_4]^-$, respectively. MO analysis of these Mo- and W-containing clusters by extended Hückel methodology has revealed that the bonding may be viewed as arising from a cationic, 26-valence electron fragment $[Pt_2(\mu\text{-}PPh_2)(PPh_3)_2]^+$ and the 18-valence electron $[CpM(CO)_3]^-$ fragment. The X-ray structures of the Pt_2Mo and Pt_3 clusters have been solved, and their structural highlights are discussed [143]. Phenylacetylene reacts readily with the trinuclear sulfido cluster $Rh(PPh_3)_2(\mu_3\text{-}S)(\mu_2\text{-}S)_3[Mo(S_2CNEt_2)]_2(\mu_2\text{-}Cl)$ to produce [Rh(SCPh=CH)Cl(PPh_3)][Mo(SCPh=CH)(S_2CNET_2)][Mo$(S_2C_2HPh)(S_2CNEt_2)$]. The insertion of the three phenylacetylene ligands into the original sulfido ligands and the formation of the bridging metallathiacyclobutene and dithiolene ligands have been ascertained by X-ray crystallography. The product contains a triangular $RhMo_2$ framework [144]. Functionalization of the charge-compensated carborane $[7\text{-}NH^tBu\text{-}\textit{nido}\text{-}7\text{-}CB_{10}H_{12}]^-$ by $Mo(CO)_6$ in refluxing MeCN produces $[1,2\text{-}\mu\text{-}NH^tBu\text{-}2,2,2\text{-}(CO)_3\text{-}\textit{closo}\text{-}2,1\text{-}MoCB_{10}H_{10}]^-$ as a relatively stable anion. The related chromium and tungsten derivatives are unstable and could only be isolated in low yields. The Mo anion reacts with $AuCl(PPh_3)$ and $[Tl][PF_6]$ to give a mixture of $1,2\text{-}\mu\text{-}NH^tBu\text{-}2\text{-}[Au(PPh_3)]\text{-}2,2,2\text{-}(CO)_3\text{-}\textit{closo}\text{-}2,1\text{-}MoCB_{10}H_{10}$ and $[N(PPh_3)_2][2,2'\text{-}\mu\text{-}Au\text{-}\{1,2\text{-}\mu\text{-}NH^tBu\text{-}2,2,2\text{-}(CO)_3\text{-}\textit{closo}\text{-}2,1\text{-}MoCB_{10}H_{10}\}_2]$. The X-ray structure of this Mo_2Au cluster (Fig. 11) reveals the presence of a linear Mo–Au–Mo unit, where a Au(I) center serves to bridge the two molybdenum centers [145].

The X-ray structure of the first silver–manganese–rhenium cluster has been reported. ReMnAg(μ-$PCy_2)(PPh_3)_2(CO)_7$ consists of a AgMnRe triangle that is bridged by a dicyclohexylphosphido unit across the

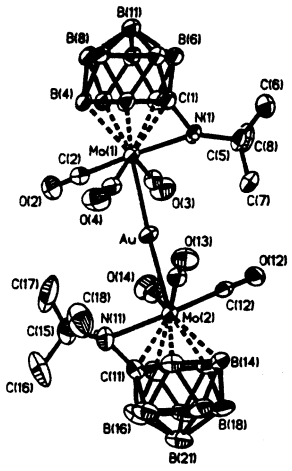

Fig. 11. X-Ray structure of [2,2′-μ-Au-{1,2-μ-NH^{t}Bu-2,2,2-(CO)$_3$-*closo*-2,1-MoCB$_{10}$H$_{10}$}$_2$]$^-$. Reprinted with permission from Inorganic Chemistry. Copyright 2001 American Chemical Society.

Re–Mn vector [146]. The inter-triangular diphosphine ligand in [AuMn$_2$(CO)$_8$(μ-PPh$_2$)]$_2$(P–P) is transformed into an intra-triangular diphosphine in AuMn$_2$(CO)$_7$(μ-PPh$_2$)(P–P) upon treatment with Me$_3$NO. The hepta-carbonyl clusters contain a bridging diphosphine ligand that serves to ligate the Au–Mn bond. The proposed mechanism for these transformations and three X-ray structures are discussed [147]. The carbyne complex [CpMn(CO)$_2$(CPh)]$^+$ was allowed to react with the diiron compounds [Fe$_2$(μ-CO)(μ-SeR)(CO)$_6$]$^-$ (where R = Ph, 4-MeC$_6$H$_4$) to furnish the trinuclear clusters MnFe$_2$(μ-H)(μ-CO)$_2$(μ$_3$-CR)(CO)$_6$(η^5-Cp). ^{1}H-NMR analysis suggests that the Fe–Fe bond is bridged by the hydride ligand. The triangular array of the MnFe$_2$ atoms, along with their capping by the benzylidyne group, has been confirmed by X-ray analysis [148]. The thiophene complex [(η^5-C$_4$H$_4$S)Ru(η^6-C$_6$Me$_6$)]$^{2+}$ reacts with Cp$_2$Co and [(1-methylnaphthalene)Mn(CO)$_3$]$^+$ at −78 °C to afford the C–S cleaved trimetallic cluster (η^6-C$_6$Me$_6$)Ru(SC$_4$H$_4$)Mn$_2$(CO)$_6$. The X-ray structure (Fig. 12) verifies the insertion of a Mn(CO)$_3$ unit into the thiophene residue, in addition to Mn–Ru bond formation in the product. The corresponding selenophene derivative reacts in an analogous fashion to give (η^6-C$_6$Me$_6$)Ru(SeC$_4$H$_4$)Mn$_2$(CO)$_6$ [149].

The heterometallic vinylidene cluster RuCo$_2$(CO)$_9$(μ$_3$-η^2-C=CHPh) undergoes Me$_3$NO-promoted CO substitution in the presence of bpcd to produce RuCo$_2$(CO)$_7$(bpcd)(μ$_3$-η^2-C=CHPh). The change in the coordination mode of the vinylidene ligand (η^2 to a Co center) and the chelation of the diphosphine ligand to the ruthenium center were established by X-ray crystallography [150]. Treatment of the diiridium complex Cp*Ir(μ-S)(μ-SCH$_2$CH$_2$CN)$_2$IrCp* with (Cp*Ru)$_4$(μ-Cl)$_4$ gives the sulfido-thiolato cluster Cp$^*_3$RuIr$_2$(μ$_3$-S)(μ-SCH$_2$CH$_2$CN)$_2$Cl. The μ$_3$-sulfido cap tethers all three metal centers, with the two bridging thiolate moieties joining the Ir and Ru centers. X-ray analysis reveals that there is only one Ru–Ir bond present in the cluster [151]. The synthesis and reactivity of (μ$_3$-C=CHPh)FeCo$_2$(CO)$_7$(dppm) and (μ$_3$-C=CHPh)FeCo$_2$(CO)$_{9-n}$L$_n$ (where L = PPh$_3$, AsPh$_3$; n = 1, 2) have been discussed. X-ray analysis shows that the dppm ligand bridges adjacent cobalt centers in the former cluster [152]. The reaction of RuCo$_2$(CO)$_{11}$ with dipropargyl malonate and terephthalate gives rise to the bis(alkyne)linked species [R(CO$_2$CH$_2$CH$_2$C$_2$H-μ$_2$][RuCo$_2$(CO)$_9$]$_2$ (where R = CH$_2$, C$_6$H$_4$-1,4). These compounds were fully characterized in solution by IR and NMR spectroscopy [153]. The bridging phosphine ligand 2,6-bis(diphenylphosphino)pyridine has been employed in the construction of new polynuclear compounds possessing Fe→Ag and Fe→Hg dative bonds.

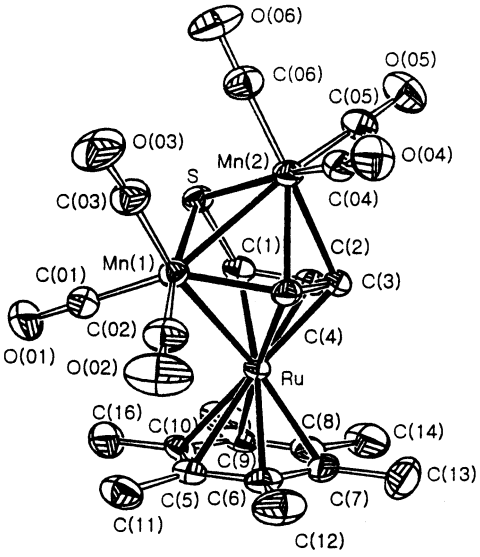

Fig. 12. X-Ray structure of (η^6-C$_6$Me$_6$)Ru(SC$_4$H$_4$)Mn$_2$(CO)$_6$. Reprinted with permission from Organometallics. Copyright 2001 American Chemical Society.

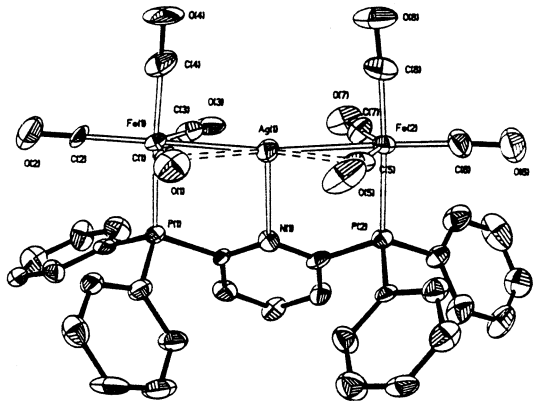

Fig. 13. X-Ray structure of [{Fe(CO)$_4$}$_2$Ag(μ-PNP)]$^+$. Reprinted with permission from Inorganic Chemistry. Copyright 2001 American Chemical Society.

Treatment of $[Fe(CO)_4]_2(\mu\text{-PNP})$ with $AgClO_4$ affords the hetero-trinuclear cluster $[\{Fe(CO)_4\}_2Ag(\mu\text{-PNP})]^+$, whose X-ray structure (Fig. 13) reveals a near linear Fe–Ag–Fe linkage. The bridging diphosphine ligand is crucial in the stabilization of the Fe→Ag dative bond. The reaction of the starting iron complex with various mercury compounds gives rise to novel Fe_2Hg_2, Fe_4Hg_8, and Fe_3Hg_4 clusters. The data from four X-ray structures are fully discussed [154].

The heterobimetallic clusters $(Cp^*Ir)_2(\mu_3\text{-S})_2MCl_2$ (where M = Pd, Pt) have been synthesized from $Cp^*IrCl(\mu\text{-SH})_2IrCpCl$ and $MCl_2(cod)$. Use of $Pd(PPh_3)_4$ in place of $PdCl_2(cod)$ gives the cationic trinuclear cluster $[(Cp^*Ir)_2(\mu_3\text{-S})_2PdCl(PPh_3)]^+$. The reactivity of the former clusters with various phosphine ligands has been investigated, with the solution NMR data presented and discussed. Both $(Cp^*Ir)_2(\mu_3\text{-S})_2MCl_2$ clusters catalyze the addition of alcohols to alkynes to produce the corresponding acetals. The X-ray structures of the three ORTEP diagrams that accompany this paper are fully discussed [155]. Linearly ordered Pt_2Rh and Pt_2Ir clusters bridged by tridentate ligands have been prepared and structurally characterized. Treatment of *syn*-$[Pt_2(\mu\text{-dpmp})_2(XylNC)_2]^{2+}$ with $[MCl(cod)]_2$ (where M = Rh, Ir) gives the linearly ordered Pt–Pt–M complexes $[Pt_2\{MCl(XylCN)_2\}(\mu\text{-dpmp})_2(XylCN)]^{2+}$. Ligand addition reactions and alkyne insertion into the Pt–Pt bond of these compounds are described. The X-ray data from six clusters are presented and fully discussed [156].

3.2. Tetranuclear clusters

The structure of $[Fe_2Ir_2(CO)_{12}]^{2-}$ has been investigated by ^{193}Ir and ^{57}Fe Mössbauer spectroscopy. The Mössbauer data of supported samples of this cluster on magnesia reveal a bimetallic structure that is molecularly physisorbed onto MgO without any transformation or decomposition. The utility of Mössbauer spectroscopy for the structural elucidation of clusters in the absence of X-ray crystallographic data is discussed [157]. The synthesis of platinum–triruthenium clusters employing the zero-valent platinum reagent $Pt(nbd)_3$ is described. Treatment of $Pt(nbd)_{3-n}(P^iPr_3)_n$ (where $n = 1, 2$), which are prepared in situ from P^iPr_3 and $Pt(nbd)_3$, with several triruthenium clusters has furnished the following structurally characterized clusters $Ru_3Pt(CO)_{11}P_2$, $Ru_3Pt(\mu\text{-H})(\mu_3\text{-}\eta^3\text{-MeCCHCMe})(CO)_9P$, $Ru_3Pt(\mu_3\text{-}\eta^2\text{-PhCCPh})(CO)_{10}P$, $Ru_3Pt(\mu\text{-H})(\mu_4\text{-N})(CO)_{10}P$, and $Ru_3Pt(\mu\text{-H})(\mu_4\text{-}\eta^2\text{-NO})(CO)_{10}P$. The structural highlights of the Ru_3Pt clusters are fully discussed [158]. The trimetallic cluster $[(MeCp)_3Mo_3S_4]^-$ reacts with $Ru(CO)_3(cod)$ and $Os(CO)_3(cod)$ to yield the heterobimetallic cubane clusters $[(MeCp)_3Mo_3S_4M(CO)_2]^-$. The ruthenium species undergoes CO loss upon standing in solution to afford the carbonyl-bridged dicubane cluster $[\{(MeCp)_3Mo_3S_4Ru\}_2(\mu\text{-CO})_3]^{2-}$, whose X-ray structure confirms the presence of a novel $Ru(\mu\text{-CO})_3Ru$ linkage. Refluxing $[(MeCp)_3Mo_3S_4]^-$ in methanol containing PPh_3 and $[M'Cl(cyclooctene)_2]_2$ (where M′ = Rh, Ir) produces the cluster compounds $[(MeCp)_3Mo_3S_4M'Cl(PPh_3)]^-$. Use of $[RhCl(cod)]_2$ in the absence of added PPh_3 gives the cod-substituted cluster $[(MeCp)_3Mo_3S_4Rh(cod)]^{2-}$. Displacement of the cod ligand by dppp yields the expected Rh-bound dppp cluster [159]. The ability of a cubane-based μ_3-S ligand to serve as a tether for a second cubane cluster has been demonstrated. The isolation, spectroscopic properties, and X-ray structure of $Fe(DMF)Cl(Cl_4\text{-cat})_2Mo_2Fe_2S_4(PEt_3)_2ClFe_4S_4Cl(PEt_3)_3(CO)_6$ are presented and discussed [160]. The tetranuclear nitrido clusters $Ru_3CoH(\mu\text{-H})(CO)_6Cp^*[\mu\text{-}\eta^2\text{-C(OMe)O}](\mu_4\text{-N})(\mu\text{-I})_2$, $Ru_3Co(\mu\text{-H})_2(CO)_6Cp^*[\mu\text{-}\eta^2\text{-C(OMe)O}](\mu_4\text{-N})I(\mu\text{-I})$ (two isomers), and $Ru_3Co(\mu\text{-H})_2(CO)_8Cp^*(\mu_4\text{-N})(\mu\text{-I})$ have been synthesized from the thermolysis of $Ru_3(\mu\text{-H})_2(CO)_9(\mu_3\text{-NOMe})$ with added $Cp^*Co(CO)I_2$. X-ray structural analyses reveal that these clusters possess either a chain (former product) or a spiked triangular core (the last three products). The ^{15}N-NMR spectra are discussed relative to the environment adopted by the ancillary nitrido ligand in these clusters [161]. The 58-electron cluster Mo_2Pd_2(2-boratanaphthalene)$(CO)_6(PEt_3)_2$ has been prepared from $[Mo(CO)_3$(2-boratanaphthalene)$]^-$ and $PdCl_2(PEt_3)_2$. X-ray analysis reveals a planar triangular core of metal atoms, where the Mo(2-boratanaphthalene)$(CO)_3$ fragments act as four-electron-donors that bridge the Pd–Pd vector. The bonding situation of the $[Mo$(2-boratanaphthalene)$(CO)_3]^-$ fragment is shown to be isolobal to the carbonyl-metallate species $[CpMo(CO)_3]^-$ [162]. The synthesis of new clusters containing the electroactive 1,4-bis-ferrocenylbutadiyne ligand has been published. The new clusters $PtOs_3(CO)_9(cod)(\mu_4\text{-FcC}_4\text{Fc})$ and $Pt_2Os_3(CO)_{10}(cod)(\mu_5\text{-FcC}_4\text{Fc})$ have been prepared from $Os_3(CO)_{10}(\mu_3\text{-FcC}_4\text{Fc})$ and $Pt(cod)_2$. The $PtOs_3$ cluster consists of a butterfly structure with the platinum atom occupying one of the wing-tip positions. A bow-tie structure has been confirmed for the Pt_2Os_3 cluster. Differential pulse voltammetry studies indicate the existence of two, one-electron oxidations for the two ferrocenyl moieties [163]. The synthesis and reactivity of $MeCpWIr_3(CO)_{11}$ are described. $[MeCpW(CO)_3]^-$ has been allowed to react with $IrCl(CO)_2$(*p*-toluidine) to afford the WIr_3 cluster in low yield. The reaction of the title cluster with diphenylacetylene gives the tetrahedral cluster $MeCpWIr_3(\mu_3\text{-}\eta^2\text{-PhC}_2\text{Ph})_2(CO)_7$, and the binuclear compound $Ir_2[\mu\text{-}\eta^4\text{-C(Ph)C(Ph)C(Ph)C(Ph)}](CO)_5$. The X-ray structures of the last two compounds reveal a common (iridacyclopentadienyl)iridium motif [164]. Treatment of $CpW(CO)_3(C{\equiv}CC{\equiv}CSiMe_3)$ with $CpRu(PPh_3)_2Cl$, followed by reaction with $Fe_2(CO)_9$, affords the tetra-

nuclear cluster $Fe_2W[\mu_3\text{-}C_2C{\equiv}C\{CpRu(PPh_3)_2\}](CO)_8Cp$. A planar Fe_2W cluster core capped by a bridging acetylide ligand has been verified by X-ray crystallography [165]. The use of $CpWRu_3(CO)_{12}(\mu\text{-H})$ in the construction of new pentanuclear clusters is described. The reaction of $CpWRu_3(CO)_{12}(\mu\text{-H})$ with $CpW(CO)_3H$ gives $Cp_2W_2Ru_3(CO)_{13}$, and which upon pyrolysis in refluxing toluene gives the oxo-carbido cluster $CpW(O)CpWRu_3(\mu_5\text{-C})(CO)_{11}$. Isotopic labeling studies suggest that a metal-assisted cleavage of a carbonyl ligand leads to the oxo and carbide ligands. Mechanistic schemes showing the CO activation and three X-ray structures are presented and fully discussed [166].

3.3. Pentanuclear clusters

$Ru_3(CO)_{12}$ reacts with $[Ir(CO)_4]^-$ to furnish the anionic cluster $[Ru_3Ir_2(CO)_{14}]^{2-}$, via the intermediate species $[Ru_3Ir(CO)_{13}]^-$. Protonation of the dianion gives $[Ru_3Ir_2(CO)_{14}H]^-$. The X-ray structure of $[Ru_3Ir_2(CO)_{14}]^{2-}$ and $[Ru_3Ir_2(CO)_{14}H]^-$ have been solved. Both structures consist of a trigonal bipyramidal metallic frame [167]. The X-ray structure of $[Re_2(CO)_8(\mu\text{-}PCy_2)]_2Pt(CO)_2$ has been determined. The two $Re_2(CO)_8(\mu\text{-}PCy_2)$ moieties are connected to the central Pt atom via the bridging of one Re–Re vector and the end-on linking of one rhenium atom of the second $Re_2(CO)_8(\mu\text{-}PCy_2)$ moiety [168]. The new mixed-metal carbide clusters $PtFe_4(CO)_{12}(cod)(\mu_5\text{-C})$ and $PtFe_4(CO)_{12}(PMe_2Ph)_2(\mu_5\text{-C})$ have been synthesized from $[Fe_5(C)(CO)_{14}]^{2-}$ and its reaction with $Cl_2Pt(cod)/TlPF_6$ and $Cl_2Pt(PMe_2Ph)_2$, respectively. Irradiation of $Fe_5(C)(CO)_{15}$ with $Pt(cod)_2$ also affords the former $PtFe_5$ cluster, but in a lower yield. Structural analyses reveal that both products consist of a square pyramidal array of metals with an interstitial carbide ligand at the center of the square base. The fluxional behavior of the PMe_2Ph ligands in the latter cluster has been studied by ^{1}H-NMR spectroscopy [169]. Thermolysis of $Fe_2W(CO)_{10}(\mu_3\text{-S})_2$ with $CpW(CO)_3(CCPh)$ gives $Fe_2(CO)_6(\mu_3\text{-S})_2W[CpW(CO)_3(CCPh)]_2$, whose X-ray structure is shown to consist of a triangular Fe_2W core that is capped by the two sulfido ligands. The acetylide ligands are attached to the core tungsten atom [170]. Mixed ruthenium/platinum clusters containing μ_4-phosphinidene and phosphorus monoxide ligands have been prepared and their transformation investigated. The capping of a Ru_3Pt face in the *nido* clusters $Ru_4(CO)_{13}(\mu_3\text{-PR})$ (where $R = N^iPr_2$, F) by the labile Pt(0) reagent $Pt(PPh_3)_2(\eta^2\text{-ethylene})$ gives $Ru_4(CO)_{12}Pt(CO)(PPh_3)(\mu_4\text{-PR})$. Acid hydrolysis of the aminophosphinidene-capped cluster yields the PO complex $[Ru_4(CO)_{12}Pt(CO)(PPh_3)(\mu_4\text{-PO})][H_2N^iPr_2]$, while ethanol reacts with the fluorophosphinidene-capped cluster to produce $Ru_4(CO)_{12}Pt(CO)(PPh_3)(\mu_4\text{-POEt})$. Four X-ray structures have been solved, and the effects of the μ_4-phosphinidene and phosphorus monoxide ligands on cluster bonding have been investigated and discussed [171]. Thermolysis of a 1:1 mixture of $Ru_3(CO)_{12}$ and $CpWRu_3(CO)_8(C_2Ph)$ (where $Cp = Cp$, Cp*) gives the carbido-alkylidyne clusters $CpWRu_4(\mu_5\text{-C})(CO)_{12}(\mu\text{-CPh})$ and $CpWRu_5(\mu_6\text{-C})(CO)_{14}(\mu\text{-CPh})$. The molecular structures of these clusters are based on a square pyramidal metal skeleton and a distorted octahedral WRu_5 framework, respectively. The hydrogenation of these clusters has been found to give $CpWRu_4(\mu_5\text{-C})(\mu\text{-CPh})(\mu\text{-H})_2(CO)_{11}$, whose X-ray structure is shown in Fig. 14, and $Cp^*WRu_5(\mu_6\text{-C})(\mu\text{-CPh})(\mu\text{-H})_2(CO)_{13}$. The activation of thiophenol by the WRu_4 carbide cluster produces $CpWRu_4(\mu_5\text{-C})(\mu\text{-CPh})(\mu\text{-H})(\mu\text{-SPh})(CO)_{11}$. Reaction schemes illustrating the reversible cleavage of the acetylide C–C bond are presented, and the VT NMR data revealing the fluxional behavior of the ancillary ligands in these clusters are discussed [172].

3.4. Hexanuclear clusters

The hexanuclear complex $(CpTi)_2(Cp^*Ru)_2Pd_2(PPh_3)(\mu_3\text{-S})_4(\mu_3\text{-O})(\mu_2\text{-H})_2$ has been obtained from $(CpTiCl)(Cp^*Ru)[Pd(PPh_3)_2](\mu_3\text{-S})(\mu_2\text{-S})(\mu_2\text{-H})_2$ upon treatment with water in the presence of a base. X-ray analysis confirms the $Ti_2Ru_2Pd_2S_4O$ core, in which two

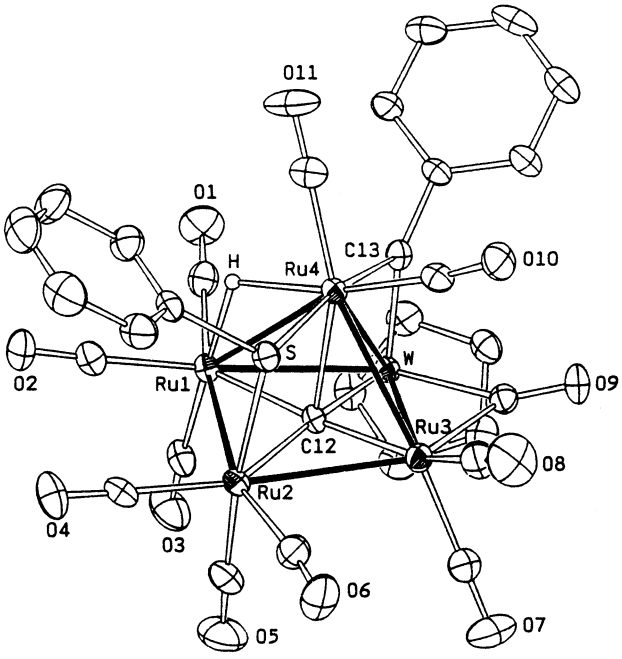

Fig. 14. X-Ray structure of $CpWRu_4(\mu_5\text{-C})(\mu\text{-CPh})(\mu\text{-H})_2(CO)_{11}$. Reprinted with permission from Organometallics. Copyright 2001 American Chemical Society.

corner-voided $TiRuPd_2S_2O$ cuboidal fragments share the Pd_2O face. The insertion of dmad into one of the Pd–S bonds gives a five-membered thiopalladatitanacycle derivative. The reaction involving the μ_3-sulfido ligand with dmad is discussed [173]. Refluxing $Mn_2(CO)_{10}$ and the nitrido cluster $[Fe_6N(CO)_{12}]^{3-}$ in EtCN or the reaction between $[Fe_4N(CO)_{12}]^-$ and $[FeMn(CO)_9]^-$ gives the anionic cluster $[Fe_5MnN(CO)_{16}]^{2-}$. The position of the Mn center in the octahedral metal frame was established by X-ray analysis. The cyclic voltammetric behavior of this Fe_5Mn cluster was examined. Cluster oxidation is followed by rapid chemical reactions that promote the decomposition of the cluster [174]. A new polymorph of $Ru_4Pt_2(CO)_{18}$ has been found by X-ray crystallography. The reaction of this cluster with added CO gives $Ru_3(CO)_{12}$ and the $[Pt(CO)]_n$ (where $n \leq 2$) [175]. A low yield of the cluster compound $W_3Ir_3(\mu_4\text{-}\eta^2\text{-}CO)(\mu\text{-}CO)(CO)_{10}(MeCp)_3$ has been obtained from the thermolysis of $W_2Ir_2(CO)_{10}(MeCp)_2$ in refluxing CH_2Cl_2. The unusual edge-bridged trigonal bipyramidal core in the product has been determined by X-ray methods. The $\mu_4\text{-}\eta^2$-CO ligand is shown to have the largest carbonyl CO bond length reported to date [176]. A report describing the high-yield syntheses of RuPt clusters has been published. The clusters $Ru_5PtC(CO)_{14}(cod)$, $Ru_5PtC(CO)_{14}(PPh_3)_2$, $Ru_5PtC(CO)_{15}(PPh_3)$, $Ru_5Pt_2C(CO)_{15}(PPh_3)_2$, $Ru_6PtC(CO)_{16}(cod)$, and $Ru_6Pt_2C(CO)_{15}(cod)_2$ have been synthesized from $[Ru_5C(CO)_{14}]^{2-}$ and $[Ru_6C(CO)_{16}]^{2-}$ and $PtCl_2L_2$. The molecular structures of all six cluster have been established by X-ray crystallography [177]. Treatment of $Ru_5(\mu_5\text{-}C_2)(\mu\text{-}SMe)_2(\mu\text{-}PPh_2)_2(CO)_{11}$ with nickelocene gives the clusters $NiRu_5(\mu_6\text{-}C_2)(\mu\text{-}SMe)_2(\mu\text{-}PPh_2)(CO)_9Cp_2$ and $Ni_2Ru_4(\mu_6\text{-}C_2)(\mu\text{-}SMe)_2(\mu\text{-}PPh_2)(CO)_8Cp_2$. The molecular structures of both products have been solved by X-ray crystallography. Extended Hückel MO calculations on the latter cluster have been carried out in order to rationalize the bonding of the dicarbide moiety to the metal framework [178]. A new mass spectrometric method for the characterization of transition metal clusters is described. The use of energy-dependent electrospray ionization mass spectrometry in the identification of reaction components has been successfully demonstrated. For example, the clusters $[Ru_5CoC(CO)_{16}]^-$, $[Ru_3Co(CO)_{13}]^-$, $[RuCo_3(CO)_{12}]^-$, $[HRu_4Co_2C(CO)_{15}]^-$, $[Ru_5IrC(CO)_{16}]^-$, $[Ru_3Ir(CO)_{13}]^-$, and $[RuIr_3(CO)_{12}]^-$, which have been found from the reaction of $Ru_6C(CO)_{17}$ with $[M(CO)_4]^-$ (where M = Co, Ir) have been fully analyzed from different reaction mixtures. Also included in this report is the X-ray structure of $[Ru_5CoC(CO)_{16}]^-$ (Fig. 15) [179].

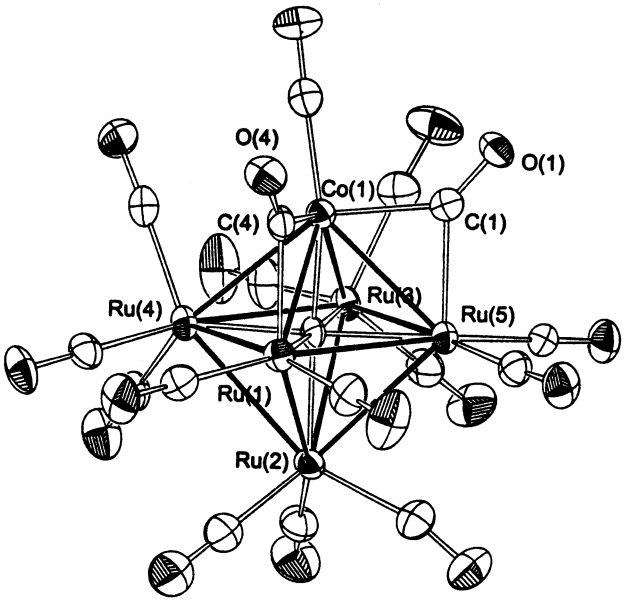

Fig. 15. X-Ray structure of $[Ru_5CoC(CO)_{16}]^-$. Reprinted with permission from Organometallics. Copyright 2001 American Chemical Society.

3.5. Higher nuclearity clusters

Infinite chains of Ru_6 clusters and silver ions have been found in the packing diagram of $[AgRu_6C(CO)_{16}]^-$, which has been synthesized from $[Ru_6C(CO)_{16}]^{2-}$ and $AgNO_3$. The self-assembly of high-nuclearity anionic clusters with cationic metal species is discussed [180]. The synthesis and molecular structures of $Au_8[Fe(CO)_4]_4(dppe)_2$ and $Au_6Cu_2[Fe(CO)_4]_4(dppe)_2$ have been published. The stereogeometry of both clusters consists of a triangulated and corrugated ribbon twisted around the elongation direction [181]. The cluster compound $[Re_7C(CO)_{21}]^{3-}$ reacts with $Hg_2(NO_3)_2$ to give $[\{Re_7C(CO)_{21}Hg\}_2]^{4-}$. The X-ray structure of this $Re_{14}Hg_2$ cluster (Fig. 16) shows that the two carbidoheptarhenate moieties are linked by a dimercury(I) unit via a face-bridging interaction. Oxidative cleavage of the Hg–Hg bond by 4-bromophenyl disulfide and halogens affords $[Re_7C(CO)_{21}HgSC_6H_4Br]^{2-}$ and $[Re_7C(CO)_{21}HgX]^{2-}$ (where X = Br, I) [182].

The new clusters $Rh_8Pt_2(CO)_{21}(dppm)_2$ and $Rh_6Pt_4(CO)_{16}(dppm)_3$ have been prepared from $[Rh_6(CO)_{15}]^{2-}/[PtCl(dppm)]_2$ and $Rh_6(CO)_{15}(MeCN)/Pt_2(CO)_3(dppm)_2$, respectively. The X-ray structures and bonding in these clusters are discussed [183]. The first example of a close-packed copper–nickel carbonyl cluster has been realized from the reaction of $[Ni_6(CO)_{12}]^{2-}$ with $CuBr_2$. Low yields of a cluster formulated as $[Cu_xNi_{35-x}(CO)_{40}]^{5-}$ (where $x = 3$ or 5) have been reported, and the molecular structure has been solved by X-ray crystallography. Structural details

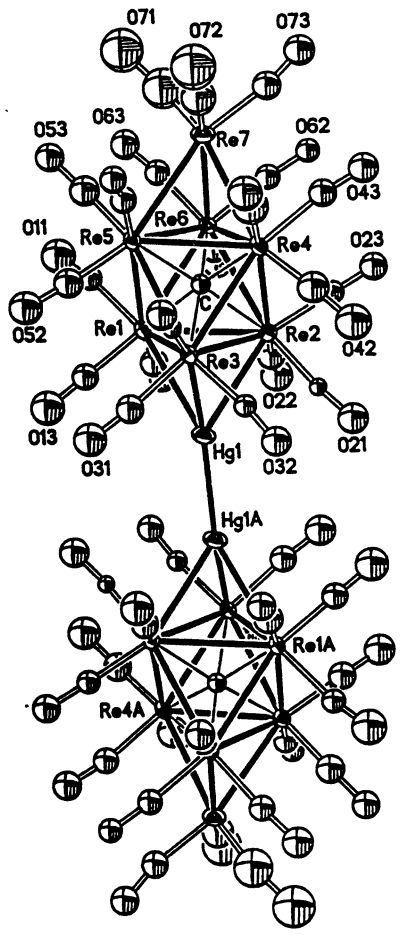

Fig. 16. X-Ray structure of $[\{Re_7C(CO)_{21}Hg\}_2]^{4-}$. Reprinted with permission from Inorganic Chemistry. Copyright 2001 American Chemical Society.

associated with this 35-atom cluster that possesses a three-layer hcp triangular stacking metal-core geometry are fully discussed [184]. New dendrimers containing up to 192 Fe_2Au cluster units have been prepared. These new materials have been synthesize from ClAu-terminated dendrimers and the anionic iron complexes $[Fe_2(CO)_7(PPh_2)]^-$ and $[Fe_3(CO)_{11}]^{2-}$ [185].

Appendix A

ampy	2-amino-6-methylpyridine
bpcd	4,5-bis(diphenylphosphino)-4-cyclopenten-1,3-dione
bpy	2,2′-bipyridine
cod	1,5-cyclooctadiene
cot	cyclooctatetraene
Cp	cyclopentadienyl
Cp*	pentamethylcyclopentadienyl
Cy	cyclohexyl
dcpm	bis(dicyclohexylphosphino)methane
dmpe	1,2-bis(dimethylphosphino)ethane
dmpm	bis(dimethylphosphino)methane
dpmp	$(Ph_2PCH_2)_2PPh$
dppa	1,2-bis(diphenylphosphino)acetylene
dppb	1,4-bis(diphenylphosphino)butane
dppe	1,2-bis(diphenylphosphino)ethane
dppf	1,1′-bis(diphenylphosphino)ferrocene
dppm	bis(diphenylphosphino)methane
dppp	1,3-bis(diphenylphosphino)propane
Fc	ferrocenyl
MAS	magic angle spinning
MeCp	methylcyclopentadienyl
nbd	norbornadiene
PPN	bis(triphenylphosphine)iminium
PTA	1,3,5-triaza-7-phosphatricyclo[3.3.1]decane
py	pyridine
Tol	tolyl
XylCN	2,6-xylyl isocyanide

References

[1] J. Sankar, Diss. Abstr. Sect. B 62 (2001) 1868 (DANQ58161).
[2] D.J. Bierdeman, Diss. Abstr. B 61 (2001) 4710 (DA9987027).
[3] C.A. Wright, Diss. Abstr. B 61 (2001) 5318 (DA9990193).
[4] M.A. Kozee, Diss. Abstr. B 61 (2001) 6467 (DA9996871).
[5] M. Shieh, L.-F. Ho, L.-F. Jang, C.-H. Ueng, S.-M. Peng, Y.-H. Liu, Chem. Commun. (2001) 1014.
[6] T. Szymańska-Buzar, T. Glowiak, I. Czeluśniak, Inorg. Chem. Commun. 4 (2001) 183.
[7] H. Brunner, F. Leis, J. Wachter, M. Zabel, J. Organomet. Chem. 627 (2001) 139.
[8] D.P. Allen, F. Bottomley, R.W. Day, A. Decken, V. Sanchez, D.A. Summers, R.C. Thompson, Organometallics 20 (2001) 1840.
[9] A.R. Dias, A. Galvão, M.H. Garcia, M.J. Villa de Brito, J. Organomet. Chem. 620 (2001) 276.
[10] M. Benito, O. Rossell, M. Seco, G. Segalés, J. Organomet. Chem. 619 (2001) 245.
[11] H. Song, Y. Lee, Z.-H. Choi, K. Lee, J.T. Park, J. Kwak, M.-G. Choi, Organometallics 20 (2001) 3139.
[12] D. Roberto, G. D'Alfonso, R. Ugo, M. Vailati, Organometallics 20 (2001) 4307.
[13] R.D. Adams, O.-S. Kwon, M.D. Smith, Inorg. Chem. 40 (2001) 5322.
[14] M. Bergamo, T. Beringhelli, G. D'Alfonso, L. Garavaglia, P. Mercandelli, M. Moret, A. Sironi, J. Clust. Sci. 12 (2001) 223.
[15] Y.A. Belousov, E.F. Brin, Polyhedron 20 (2001) 2765.
[16] E. Gatto, G. Gervasio, D. Marabello, E. Sappa, J. Chem. Soc. Dalton Trans. (2001) 1485.
[17] N.E. Leadbeater, C. van der Pol, Chem. Commun. (2001) 599.
[18] H. Bielawa, O. Hinrichsen, A. Birkner, M. Muhler, Angew. Chem. Int. Ed. 40 (2001) 1061.
[19] F. Kakiuchi, K. Igi, M. Matsumoto, N. Chatani, S. Murai, Chem. Lett. (2001) 422.
[20] N. Chatani, T. Asaumi, S. Yorimitsu, T. Ikeda, F. Kakiuchi, S. Murai, J. Am. Chem. Soc. 123 (2001) 10935.
[21] D. Berger, A. Göbel, W. Imhof, J. Mol. Catal. A 165 (2001) 37.
[22] G. Liu, M. Hakimifard, M. Garland, J. Mol. Catal. A 168 (2001) 33.

[23] T. Kondo, T. Okada, T. Suzuki, T. Mitsudo, J. Organomet. Chem. 622 (2001) 149.
[24] C.S. Cho, B.T. Kim, M.J. Lee, T.-J. Kim, S.C. Shim, Angew. Chem. Int. Ed. 40 (2001) 958.
[25] A. Göbel, W. Imhof, Chem. Commun. (2001) 593.
[26] F. Ragaini, S. Cenini, M. Gasperini, J. Mol. Catal. A 174 (2001) 51.
[27] K. Dallmann, R. Buffon, J. Mol. Catal. A 172 (2001) 81.
[28] Y. Chi, J.-W. Lan, S.-M. Peng, G.-H. Lee, J. Clust. Sci. 12 (2001) 421.
[29] Y. Zhang, B. Wang, S. Xu, X. Zhou, Organometallics 20 (2001) 3829.
[30] X. Lei, M. Shang, T.P. Fehlner, Organometallics 20 (2001) 1479.
[31] D.A. McCarthy, H.E. Durie, J.J. Embry, L.A. Imbur, K.A. Marhoefer, Inorg. Chem. 40 (2001) 1972.
[32] M.I. Bruce, B.W. Skelton, A. Werth, A.H. White, Aust. J. Chem. 54 (2001) 93.
[33] J.P.H. Charmant, P.J. King, R. Quesada-Pato, E. Sappa, C. Schaefer, J. Chem. Soc. Dalton Trans. (2001) 46.
[34] A.J. Amoroso, L.P. Clarke, J.E. Davies, J. Lewis, H.R. Powell, P.R. Raithby, G.P. Shields, J. Organomet. Chem. 635 (2001) 119.
[35] R.D. Adams, O.-S. Kwon, B. Qu, M.D. Smith, Organometallics 20 (2001) 5225.
[36] M.I. Bruce, A.C. Meier, B.W. Skelton, A.H. White, N.N. Zaitseva, Aust. J. Chem. 54 (2001) 319.
[37] S. Brait, S. Deabate, S.A.R. Knox, E. Sappa, J. Clust. Sci. 12 (2001) 139.
[38] H. Song, K. Lee, C.H. Lee, J.T. Park, H.Y. Chang, M.-G. Choi, Angew. Chem. Int. Ed. 40 (2001) 1500.
[39] M.W. Lum, W.K. Leong, J. Chem. Soc. Dalton Trans. (2001) 2476.
[40] T. Castrillo, L. D'Ornelas, L. Hernández, M. Orea, R. Atencio, S. Pekerar, Inorg. Chim. Acta 319 (2001) 207.
[41] S. Aime, A.J. Arce, O. Chiantore, R. Gobetto, A. Russo, Y. De Sanctis, J. Organomet. Chem. 622 (2001) 43.
[42] E. Lucenti, D. Roberto, R. Ugo, Organometallics 20 (2001) 1725.
[43] S. Aime, W. Dastrú, R. Gobetto, F. Reineri, A. Russo, A. Viale, Organometallics 20 (2001) 2924.
[44] S.P. Tunik, V.D. Khripun, I.A. Balova, E. Nordlander, M. Haukka, T.A. Pakkanen, P.R. Raithby, Organometallics 20 (2001) 3854.
[45] S.F.A. Kettle, E. Diana, R. Rossetti, P.L. Shanghellini, Inorg. Chim. Acta 319 (2001) 75.
[46] M. Faure, A.T. Vallina, H. Stoeckli-Evans, G. Süss-Fink, J. Organomet. Chem. 621 (2001) 103.
[47] A.J. Arce, Y. De Sanctis, E. Galarza, M.T. Garland, R. Gobetto, R. Machado, J. Manzur, A. Russo, E. Spodine, M.J. Stchedroff, Organometallics 20 (2001) 359.
[48] R. Okamura, K. Tada, K. Matsubara, M. Oshima, H. Suzuki, Organometallics 20 (2001) 4772.
[49] T. Takemori, A. Inagaki, H. Suzuki, J. Am. Chem. Soc. 123 (2001) 1762.
[50] J.A. Cabeza, M. Moreno, V. Riera, M. de, J. Rosales-Hoz, Inorg. Chem. Commun. 4 (2001) 57.
[51] R.D. Adams, B. Qu, M.D. Smith, J. Organomet. Chem. 637–639 (2001) 514.
[52] J.A. Cabeza, I. del Río, S. García-Granda, M. Moreno, V. Riera, Organometallics 20 (2001) 4973.
[53] J.-Y. Saillard, S. Kahlal, V. Ferrand, H. Stoeckli-Evans, G. Süss-Fink, J. Organomet. Chem. 620 (2001) 119.
[54] M.I. Alcalde, A.J. Carty, Y. Chi, E. Delgado, B. Donnadieu, E. Hernández, K. Dallmann, J. Sánchez-Nieves, J. Chem. Soc. Dalton Trans. (2001) 2502.
[55] N.K. Kiriakidou-Kazemifar, E. Kretzschmar, H. Carlsson, M. Monari, S. Selva, E. Nordlander, J. Organomet. Chem. 623 (2001) 191.
[56] A.L. Eckermann, D. Fenske, T.B. Rauchfuss, Inorg. Chem. 40 (2001) 1459.
[57] C.S. Allardyce, P.J. Dyson, J. Clust. Sci. 12 (2001) 563.
[58] N.T. Lucas, M.P. Cifuentes, L.T. Nguyen, M.G. Humphrey, J. Clust. Sci. 12 (2001) 201.
[59] W.K. Leong, W.L.J. Leong, J. Zhang, J. Chem. Soc. Dalton Trans. (2001) 1087.
[60] S.-G. Ang, X. Zhong, H.-G. Ang, J. Chem. Soc. Dalton Trans. (2001) 1151.
[61] W.-Y. Wong, F.-L. Ting, W.-L. Lam, J. Chem. Soc. Dalton Trans. (2001) 2981.
[62] D. Blazina, S.B. Duckett, P.J. Dyson, B.F.G. Johnson, J.A.B. Lohman, C.J. Sleigh, J. Am. Chem. Soc. 123 (2001) 9760.
[63] C.J. Adams, M.I. Bruce, P.A. Humphrey, B.W. Skelton, A.H. White, Aust. J. Chem. 54 (2001) 325.
[64] H. Adams, S.C.M. Agustinho, K. Chomka, B.E. Mann, S. Smith, C. Squires, S.E. Spey, Can. J. Chem. 79 (2001) 760.
[65] D. Cauzzi, C. Graiff, C. Massera, G. Predieri, A. Tiripicchio, J. Clust. Sci. 12 (2001) 259.
[66] H.-C. Böttcher, M. Graf, K. Merzweiler, T. Rösel, H. Schmidt, C. Wagner, Polyhedron 20 (2001) 2011.
[67] F.F. de Biani, C. Graiff, G. Opromolla, G. Predieri, A. Tiripicchio, P. Zanello, J. Organomet. Chem. 637–639 (2001) 586.
[68] E.N.-M. Ho, B.K.-M. Hui, W.-T. Wong, J. Organomet. Chem. 637-639 (2001) 276.
[69] G. Süss-Fink, I. Godefroy, M. Faure, A. Neels, H. Stoeckli-Evans, J. Clust. Sci. 12 (2001) 35.
[70] E.L. Diz, A. Neels, H. Stoeckli-Evans, G. Süss-Fink, Polyhedron 20 (2001) 2771.
[71] M.I. Bruce, B.W. Skelton, A.H. White, N.N. Zaitseva, J. Chem. Soc. Dalton Trans. (2001) 355.
[72] C.T. Tay, W.K. Leong, J. Organomet. Chem. 625 (2001) 231.
[73] W.K. Leong, G. Chen, Organometallics 20 (2001) 2280.
[74] D.J. Bierdeman, J.B. Keister, D.A. Jelski, J. Organomet. Chem. 633 (2001) 51.
[75] S.M.T. Abedin, K.A. Azam, M.B. Hursthouse, S.E. Kabir, K.M.A. Malik, M.A. Mottalib, E. Rosenberg, J. Clust. Sci. 12 (2001) 5.
[76] O.A. Kizas, V.V. Krivykh, E.V. Vorontsov, O.L. Tok, F.M. Dolgushin, A.A. Koridze, Organometallics 20 (2001) 4170.
[77] S.E. Kabir, C.A. Johns, K.M.A. Malik, M.A. Mottalib, E. Rosenberg, J. Organomet. Chem. 625 (2001) 112.
[78] R. Persson, M. Monari, R. Gobetto, A. Russo, S. Aime, M.J. Calhorda, E. Nordlander, Organometallics 20 (2001) 4150.
[79] S.M. Yunusov, E.S. Kalyuzhnaya, B.L. Moroz, S.N. Agafonova, V.A. Likholobov, V.B. Shur, J. Mol. Catal. A 165 (2001) 141.
[80] H. Kondo, Y. Yamaguchi, H. Nagashima, J. Am. Chem. Soc. 123 (2001) 500.
[81] F. Chérioux, A. Maisse-Francois, A. Neels, H. Stoeckli-Evans, G. Süss-Fink, J. Chem. Soc. Dalton Trans. (2001) 2184.
[82] P.J. Dyson, K. Russell, T. Welton, Inorg. Chem. Commun. 4 (2001) 571.
[83] R.D. Adams, B. Qu, J. Organomet. Chem. 619 (2001) 271.
[84] Y. Li, W.-T. Wong, J. Clust. Sci. 12 (2001) 595.
[85] J.A. Cabeza, I. del Río, F. Grepioni, M. Moreno, V. Riera, M. Suárez, Organometallics 20 (2001) 4190.
[86] S. Kahlal, W. Wang, L. Scoles, K.A. Udachin, J.-Y. Saillard, A.J. Carty, Organometallics 20 (2001) 4469.
[87] C.E. Housecroft, D.M. Nixon, A.L. Rheingold, J. Clust. Sci. 12 (2001) 89.
[88] F. Jiang, G.P.A. Yap, R.K. Pomeroy, J. Clust. Sci. 12 (2001) 433.

[89] K. Lee, Z.-H. Choi, Y.-J. Cho, H. Song, J.T. Park, Organometallics 20 (2001) 5564.
[90] C.M.G. Judkins, K.A. Knights, B.F.G. Johnson, Y.R. de Miguel, R. Raja, J.M. Thomas, Chem. Commun. (2001) 2624.
[91] S. Hermans, R. Raja, J.M. Thomas, B.F.G. Johnson, G. Sankar, D. Gleeson, Angew. Chem. Int. Ed. 40 (2001) 1211.
[92] P.J. Dyson, A.K. Hearley, B.F.G. Johnson, J.S. McIndoe, P.R.R. Langridge-Smith, J. Clust. Sci. 12 (2001) 273.
[93] W.K. Leong, G. Chen, Organometallics 20 (2001) 5771.
[94] E. Lucenti, D. Roberto, C. Roveda, R. Ugo, E. Cariati, J. Clust. Sci. 12 (2001) 113.
[95] X. Fan, R. Cao, M. Hong, W. Su, D. Sun, J. Chem. Soc. Dalton Trans. (2001) 2961.
[96] T. Sugihara, A. Wakabayashi, H. Takao, H. Imagawa, M. Nishizawa, Chem. Commun. (2001) 2456.
[97] K.W. Muir, R. Rumin, F.Y. Pétillon, J. Organomet. Chem. 635 (2001) 110.
[98] H. Brunner, F. Leis, J. Wachter, M. Zabel, J. Organomet. Chem. 628 (2001) 39.
[99] F.H. Försterling, C.E. Barnes, J. Organomet. Chem. 617–618 (2001) 561.
[100] S.G. Bott, H. Shen, M.G. Richmond, Struct. Chem. 12 (2001) 225.
[101] F. Gelman, D. Avnir, H. Schumann, J. Blum, J. Mol. Catal. A 171 (2001) 191.
[102] A.M. Argo, J.F. Goellner, B.L. Phillips, G.A. Panjabi, B.C. Gates, J. Am. Chem. Soc. 123 (2001) 2275.
[103] H. Wadepohl, R. Merkel, H. Pritzkow, S. Rihm, J. Chem. Soc. Dalton Trans. (2001) 3617.
[104] C. Tejel, M.A. Ciriano, B.E. Villarroya, R. Gelpi, J.A. López, F.J. Lahoz, L.A. Oro, Angew. Chem. Int. Ed. 40 (2001) 4084.
[105] B.E. Hodson, D. Ellis, T.D. McGrath, J.J. Monaghan, G.M. Rosair, A.J. Welch, Angew. Chem. Int. Ed. 40 (2001) 715.
[106] M.I. Bruce, A.J. Carty, B.G. Ellis, P.J. Low, B.W. Skelton, A.H. White, K.A. Udachin, N.N. Zaitseva, Aust. J. Chem. 54 (2001) 277.
[107] R.M. De Silva, M.J. Mays, P.R. Raithby, G.A. Solan, J. Organomet. Chem. 625 (2001) 245.
[108] R.D. Pergola, L. Garlaschelli, M. Manassero, M. Sansoni, D. Strumolo, J. Clust. Sci. 12 (2001) 23.
[109] H. Lang, G. Rheinwald, U. Lay, L. Zsolnai, G. Huttner, J. Organomet. Chem. 634 (2001) 74.
[110] D.H. Farrar, E.V. Grachova, A. Lough, C. Patirana, A.J. Pöe, S.P. Tunik, J. Chem. Soc. Dalton Trans. (2001) 2015.
[111] E.V. Grachova, B.T. Heaton, J.A. Iggo, I.S. Podkorytov, D.J. Smawfield, S.P. Tunik, R. Whyman, J. Chem. Soc. Dalton Trans. (2001) 3303.
[112] J.S.Z. Sabounchei, B.T. Heaton, J.A. Iggo, C. Jacob, I.S. Podkorytov, J. Clust. Sci. 12 (2001) 339.
[113] G. Ciani, A. Sironi, S. Martinengo, L. Garlaschelli, R.D. Pergola, P. Zanello, F. Laschi, N. Masciocchi, Inorg. Chem. 40 (2001) 3905.
[114] R. Ros, A. Tassan, R. Roulet, V. Duprez, S. Detti, G. Laurenczy, K. Schenk, J. Chem. Soc. Dalton Trans. (2001) 2858.
[115] S. Bhaduri, G.K. Lahiri, D. Mukesh, H. Paul, K. Sarma, Organometallics 20 (2001) 3329.
[116] R. Ros, G. Facchin, A. Tassan, R. Roulet, G. Laurenczy, F. Lukacs, J. Clust. Sci. 12 (2001) 99.
[117] D. Brevet, D. Lucas, H. Cattey, F. Lemaître, Y. Mugnier, P.D. Harvey, J. Am. Chem. Soc. 123 (2001) 4340.
[118] A. Fortunelli, P. Leoni, L. Marchetti, M. Pasquali, F. Sbrana, M. Selmi, Inorg. Chem. 40 (2001) 3055.
[119] E. Alonso, J.M. Casas, J. Forniés, C. Fortuño, A. Martín, A.G. Orpen, C.A. Tsipis, A.C. Tsipis, Organometallics 20 (2001) 5571.
[120] E. Alonso, J. Forniés, C. Fortuño, A. Martín, A.G. Orpen, Organometallics 20 (2001) 850.
[121] T. Tanase, R.A. Begum, Organometallics 20 (2001) 106.
[122] B.T. Sterenberg, R. Ramachandran, R.J. Puddephatt, J. Clust. Sci. 12 (2001) 49.
[123] P. Leoni, F. Marchetti, L. Marchetti, M. Pasquali, S. Quaglierini, Angew. Chem. Int. Ed. 40 (2001) 3617.
[124] L.R. Falvello, J. Forniés, J. Gómez, E. Lalinde, A. Martín, F. Martínez, M.T. Moreno, J. Chem. Soc. Dalton Trans. (2001) 2132.
[125] F. Demartin, F.F. de Biani, C. Femoni, M.C. Iapalucci, G. Longoni, P. Macchi, P. Zanello, J. Clust. Sci. 12 (2001) 61.
[126] N.T. Tran, M. Kawano, L.F. Dahl, J. Chem. Soc. Dalton Trans. (2001) 2731.
[127] C. Femoni, M.C. Iapalucci, G. Longoni, P.H. Svensson, Chem. Commun. (2001) 1776.
[128] M. Kawano, J.W. Bacon, C.F. Campana, B.E. Winger, J.D. Dudek, S.A. Sirchio, S.L. Scruggs, U. Geiser, L.F. Dahl, Inorg. Chem. 40 (2001) 2554.
[129] V.W.-W. Yam, C.-H. Lam, K.-K. Cheung, Inorg. Chim. Acta 316 (2001) 19.
[130] E.J. Fernández, M. Gil, M.E. Olmos, O. Crespo, A. Laguna, P.G. Jones, Inorg. Chem. 40 (2001) 3018.
[131] S. Canales, O. Crespo, M.C. Gimeno, P.G. Jones, A. Laguna, F. Mendizabal, Organometallics 20 (2001) 4812.
[132] D. Rais, J. Yau, D.M.P. Mingos, R. Vilar, A.J.P. White, D.J. Williams, Angew. Chem. Int. Ed. 40 (2001) 3464.
[133] S. Kuwata, S.-I. Kabashima, N. Sugiyama, Y. Ishii, M. Hidai, Inorg. Chem. 40 (2001) 2034.
[134] M. Yuki, M. Okazaki, H. Ogino, Organometallics 20 (2001) 1762.
[135] L.-C. Song, C.-C. Luo, Q.-M. Hu, J. Chen, H.-G. Wang, Organometallics 20 (2001) 4510.
[136] L.-C. Song, Q.-S. Li, Q.-M. Hu, Y.-B. Dong, J. Organomet. Chem. 619 (2001) 194.
[137] L.-C. Song, D.-S. Guo, Q.-M. Hu, F.-H. Su, J. Sun, X.-Y. Huang, J. Organomet. Chem. 622 (2001) 210.
[138] L.-C. Song, Q.-S. Li, Q.-M. Hu, C.-C. Luo, Y.-B. Dong, Inorg. Chim. Acta 314 (2001) 63.
[139] Y.-H. Zhang, J.-C. Yuan, Y.-Q. Yin, Z.-Y. Zhou, A.S.C. Chan, Polyhedron 20 (2001) 1859.
[140] A.J. Bridgeman, M.J. Mays, A.D. Woods, Organometallics 20 (2001) 2932.
[141] M. Scheer, S.B. Umbarkar, S. Chatterjee, R. Trivedi, P. Mathur, Angew. Chem. Int. Ed. 40 (2001) 376.
[142] P. Braunstein, M.J. Chetcuti, R. Welter, Chem. Commun. (2001) 2508.
[143] C. Archambault, R. Bender, P. Braunstein, S.-E. Bouaoud, D. Rouag, S. Golhen, L. Ouahab, Chem. Commun. (2001) 849.
[144] T. Ikada, Y. Mizobe, M. Hidai, Organometallics 20 (2001) 4441.
[145] S. Du, J.A. Kautz, T.D. McGrath, F.G.A. Stone, Inorg. Chem. 40 (2001) 6563.
[146] U. Flörke, D. Petters, Acta Crystallogr. C57 (2001) 1044.
[147] K.H. Lee, P.M.N. Low, T.S.A. Hor, Y.-S. Wen, L.K. Liu, Organometallics 20 (2001) 3250.
[148] R. Wang, Q. Xu, Y. Souma, L.-C. Song, J. Sun, J. Chen, Organometallics 20 (2001) 2226.
[149] D.S. Choi, I.S. Lee, S.U. Son, Y.K. Chung, Organometallics 20 (2001) 3617.
[150] S.G. Bott, H. Shen, M.G. Richmond, Struct. Chem. 12 (2001) 237.
[151] F. Takagi, H. Seino, Y. Mizobe, M. Hidai, Can. J. Chem. 79 (2001) 632.
[152] Q.L. Suo, H. Zhang, Y. Wang, L. Wang, L. Wen, X. Leng, J. Organomet. Chem. 631 (2001) 87.
[153] Y.-H. Zhang, W.-J. Lao, Y.-Q. Liu, Y.-Q. Yin, J.-J. Wu, Z.-X. Huang, Polyhedron 20 (2001) 1107.
[154] H.-B. Song, Z.-Z. Zhang, T.C.W. Mak, Inorg. Chem. 40 (2001) 5928.

[155] D. Masui, T. Kochi, Z. Tang, Y. Ishii, Y. Mizobe, M. Hidai, J. Organomet. Chem. 620 (2001) 69.
[156] T. Tanase, R.A. Begum, H. Toda, Y. Yamamoto, Organometallics 20 (2001) 968.
[157] L. Stievano, S. Calogero, R. Psaro, M. Guidotti, R.D. Pergola, F.E. Wagner, J. Clust. Sci. 12 (2001) 123.
[158] D. Ellis, L.J. Farrugia, J. Clust. Sci. 12 (2001) 243.
[159] K. Herbst, M. Monari, M. Brorson, Inorg. Chem. 40 (2001) 2979.
[160] J. Han, D. Coucouvanis, J. Am. Chem. Soc. 123 (2001) 11304.
[161] E.N.-M. Ho, W.-T. Wong, J. Organomet. Chem. 626 (2001) 125.
[162] P. Braunstein, E. Cura, G.E. Herberich, J. Chem. Soc. Dalton Trans. (2001) 1754.
[163] R.D. Adams, B. Qu, J. Organomet. Chem. 620 (2001) 303.
[164] E.G.A. Notaras, N.T. Lucas, J.P. Blitz, M.G. Humphrey, J. Organomet. Chem. 631 (2001) 143.
[165] M.I. Bruce, P.J. Low, M. Ke, B.D. Kelly, B.W. Skelton, M.E. Smith, A.H. White, N.B. Witton, Aust. J. Chem. 54 (2001) 453.
[166] Y. Chi, S.-M. Peng, G.-H. Lee, C.-J. Su, Organometallics 20 (2001) 1102.
[167] A. Fumagalli, M.C. Malatesta, M. Vallario, G. Ciani, M. Moret, A. Sironi, J. Clust. Sci. 12 (2001) 187.
[168] H.-J. Haupt, U. Flörke, S. Klose, Acta Crystallogr. C57 (2001) 810.
[169] R.D. Adams, B. Captain, W. Fu, J. Clust. Sci. 12 (2001) 303.
[170] P. Mathur, S. Mukhopadhyay, M.O. Ahmed, G.K. Lahiri, S. Chakraborty, V.G. Puranik, M.M. Bhadbhade, S.B. Umbarkar, J. Organomet. Chem. 629 (2001) 160.
[171] L. Scoles, J.H. Yamamoto, L. Brissieux, B.T. Sterenberg, K.A. Udachin, A.J. Carty, Inorg. Chem. 40 (2001) 6731.
[172] S.-F. Hwang, Y. Chi, S.-J. Chiang, S.-M. Peng, G.-H. Lee, Organometallics 20 (2001) 215.
[173] S. Kumata, S. Kabashima, Y. Ishii, M. Hidai, J. Am. Chem. Soc. 123 (2001) 3826.
[174] R.D. Pergola, L. Garlaschelli, M. Manassero, M. Sansoni, D. Strumolo, F.F. de Biani, P. Zanello, J. Chem. Soc. Dalton Trans. (2001) 2179.
[175] V. Antonucci, A.S. Aricò, F. Calderazzo, L. Labella, F. Marchetti, J. Clust. Sci. 12 (2001) 293.
[176] E.G.A. Notaras, N.T. Lucas, M.G. Humphrey, J. Organomet. Chem. 631 (2001) 139.
[177] S. Hermans, T. Khimyak, B.F.G. Johnson, J. Chem. Soc. Dalton Trans. (2001) 3295.
[178] C.J. Adams, M.I. Bruce, J.-F. Halet, S. Kahlal, B.W. Skelton, A.H. White, J. Chem. Soc. Dalton Trans. (2001) 414.
[179] P.J. Dyson, A.K. Hearley, B.F.G. Johnson, T. Khimyak, J.S. McIndoe, P.R.R. Langridge-Smith, Organometallics 20 (2001) 3970.
[180] T. Nakajima, A. Ishiguro, Y. Wakatsuki, Angew. Chem. Int. Ed. 40 (2001) 1066.
[181] V.G. Albano, C. Castellari, C. Femoni, M.C. Iapalucci, G. Longoni, M. Monari, S. Zacchini, J. Clust. Sci. 12 (2001) 75.
[182] C.A. Wright, U. Brand, J.R. Shapley, Inorg. Chem. 40 (2001) 4896.
[183] I.O. Koshevoy, S.P. Tunik, S. Jääskeläinen, M. Haukka, T.A. Pakkanen, J. Chem. Soc. Dalton Trans. (2001) 2965.
[184] P.D. Mlynek, M. Kawano, M.A. Kozee, L.F. Dahl, J. Clust. Sci. 12 (2001) 313.
[185] M. Benito, O. Rossell, M. Seco, G. Segalés, V. Maraval, R. Laurent, A.-M. Caminade, J.-P. Majoral, J. Organomet. Chem. 622 (2001) 33.